SLAC – PUB – 4039 (REV)
January 1988
(T/E)

ELECTROWEAK RADIATIVE CORRECTIONS WITH AN EFFECTIVE LAGRANGIAN: FOUR-FERMION PROCESSES*

D. C. KENNEDY AND B. W. LYNN

Institute for Theoretical Physics, Department of Physics

and

Stanford Linear Accelerator Center

Stanford University, Stanford, California 94305

Abstract

We present a new and more concise method for computing and organizing electroweak radiative corrections, based on an effective Lagrangian and incorporating a large class of diagrams into a few simple running couplings without use of truncated renormalization group approximations. We apply this technique to the case of four-fermion processes. Special emphasis is placed on the effects of heavy particles on low-energy physics and how such phenomena can be classified and measured in the new generation of precision electroweak experiments — in particular, experiments with polarized e^- beams at the SLC and LEP.

Submitted to Nuclear Physics B

* Work supported by the Department of Energy, contract DE – AC03 – 76SF00515.

1. Introduction

The approach of the SLC/LEP era brings with it the promise of accurate tests of electroweak physics, especially of the physics of radiative corrections. These corrections to electroweak processes (such as e^+e^- collisions) are an integral part of the field theory of the standard Glashow–Salam–Weinberg model and its various extensions. Hence, they are essential to checking in detail the validity of electroweak theories. Although a great deal of work has been done on electroweak radiative corrections, a comprehensive and self-consistent treatment of their effects is lacking. The present paper is a complete reformulation of electroweak virtual corrections, applied in particular to four-fermion processes and incorporated into a simple and consistent theoretical structure using an *effective Lagrangian.*

There are a number of basic difficulties with radiative corrections. The complexity of the model and the large number of Feynman diagrams to be included in a complete calculation have often led in past treatments to obscurity, with no clear physical relationship between the radiative corrections and the quantities being corrected. A subclass of the corrections, moreover, contains infinities that must be removed, or renormalized, to recover a meaningful theory. The renormalization procedure eliminates the divergences and relates the original, or *bare,* parameters of the theory to the physical, or *renormalized,* ones. A renormalizable theory is definable if, given a finite number of experimental inputs, any physical quantity is computable in a finite, sensible way. Any given set of inputs is called a *Renormalization Scheme* (RS). The obscurity of most radiative correction methods, when combined with conventional renormalization techniques, on occasion has also given rise to problematic self-inconsistencies, *RS-dependence.*[1] That is, physical quantities such as cross sections are found to depend on the set of inputs used to define the theory.

The approach developed in this paper generates a new way of organizing and thinking about radiative corrections, one that can take full advantage of the

gauge symmetry of the electroweak theory and its manifold consequences. This method greatly simplifies the incorporation of radiative corrections into electroweak processes. It organizes them in an essentially unique way, one that is fixed by the physical symmetries of the theory and that eliminates most of the arbitrariness and all of the inconsistencies potentially present in their renormalization. To be concise, we will call the result the *RS–independent* representation of an electroweak process. Quantum electrodynamics (QED) will be used first as a warm-up exercise in Section 2 to illustrate the idea, which will then be extended to the full electroweak theory in Section 3. To demonstrate the simplicity achieved in the treatment of radiative corrections, Sections 4 and 5 provide a general review of the physics of virtual corrections in the standard model, organized in a comprehensive and unified manner. We stress in particular the effect of the nondecoupling of heavy particles in low-energy physics. The potential uncovering of physics beyond the standard model via radiative corrections becomes the main theme of Section 6. The power of the RS–independent representation is especially evident here, as it renders unambiguous the kind of "heavy physics" that can be learned from radiative corrections and the relationship between electroweak experiments at different energies. We use the Euclidean metric throughout, $q^2 = \vec{q}^2 - q_0^2$.

2. Renormalization Scheme–Independence of QED

We begin by showing how the general QED matrix element can be made manifestly RS–independent. The loop corrections in QED can be classified into a number of groups: gauge boson propagator ("oblique") corrections (Fig. 1) and "direct" corrections: vertices, boxes and bremsstrahlung[2] (Fig. 2). Each of these four groups is a gauge-invariant subset and so can be treated separately. We concentrate mainly on the "oblique" or vacuum polarization corrections. The other corrections are process-specific, in that they depend on the external particle masses and quantum numbers, as well as the specific experimental arrangement. The oblique corrections are universal, as the appear in any process mediated by photons.

The vacuum polarization of Fig. 1 is of course infinite. The general method of eliminating, or "renormalizing," these infinities in common use is the "counterterm" approach, most often associated with Bogoliubov, Parasiuk, Hepp and Zimmermann (BPHZ).[3] In this method, one begins calculations with the "renormalized" classical Lagrangian $\mathcal{L}_{ren}$. Infinities are then eliminated order by order in the perturbation theory by adding to $\mathcal{L}_{ren}$ counterterms designed to cancel any divergent parts of Feynman graphs. $\mathcal{L}_{ren}$ is expressed in terms of "renormalized," or finite, fields and parameters. The collection of necessary counterterms is called the *counterterm* Lagrangian, $\mathcal{L}_{ct}$, and the result of the perturbative renormalization is the *bare* Lagrangian, $\mathcal{L}_0 \equiv \mathcal{L}_{ren} + \mathcal{L}_{ct}$, expressed in terms of the so-called bare fields and parameters, themselves functions of the renormalized field and parameters.

The crucial point about counterterm renormalization is that the counterterms are arbitrary; apart from the infinite terms, one can cancel any finite part from any Feynman graphs that one desires. In addition, $\mathcal{L}_{ren}$ is arbitrary, in spite of its name; only the combination $\mathcal{L}_0 \equiv \mathcal{L}_{ren} + \mathcal{L}_{ct}$ is physically meaningful. In fact, the true classical Lagrangian of Nature *is* the bare Lagrangian; any results based on it are finite and unambiguous. It is only the division of $\mathcal{L}_0$

into "renormalized" terms and "counterterms" that is arbitrary; each way of making this division corresponds to a different RS, defining in each case a set of "renormalized" fields and parameters (in $\mathcal{L}_{ren}$) and a set of counterterms (in $\mathcal{L}_{ct}$). In the counterterm approach one can make RS–independence manifest in the end by using renormalization group (RNG) invariance. The quantitative consequence is the RNG equation, through which one can introduce "running" parameters analogous to the ones presented in this paper.[4] A serious practical difficulty with the RNG equation, which comes in a number of versions, is in obtaining anything but asymptotic (leading logarithm) behavior from it.[3] The Callan–Symanzik equation is tractable only in the high-energy limit; the minimal subtraction RNG equation is exactly soluble, but in order to get nonasymptotic behavior out of it, one needs to compute various loop integrals exactly anyway. In strong interaction physics, with light quarks, this difficulty poses no problems; in electroweak physics at energies below a few hundred GeV, mass threshold effects are of decisive importance. The RNG approach, by itself, would therefore seem to be of quite limited usefulness, while complete calculations of radiative corrections have generally been complicated and opaque. A fresh approach to radiative corrections would retain the simplicity of the RNG, while being fully up to the complexity of a broken gauge theory with mixing and mass thresholds. Such a new approach should also be unified and comprehensive.

A major conceptual and practical simplification of electroweak and other calculations ensues if we take a different tack and return to the original field theory methods of Feynman, Schwinger and Dyson:[5] since the bare Lagrangian $\mathcal{L}_0$ is the true classical Lagrangian, it is the logical place begin a calculation. One can then imagine using $\mathcal{L}_0$ in the path integral and generating the *effective action,* or the *effective Lagrangian,* $\mathcal{L}_{eff}$, which contains all of the quantum corrections and is expressed in terms of bare parameters and fields. The effective action serves as a complete description of a physical system. It is computable order by order in perturbation theory, as exemplified by the approach of Coleman and Weinberg,[6] who calculated the effective potential of the vacuum in the $\lambda\phi^4$ theory to one

loop. In the present case, we need the effective Lagrangian for the S–matrix; i.e., for transitions between states of definite incoming and outgoing particles. The effective Lagrangian also appears in other contexts, computed in different approximations, such as the chiral Lagrangian of low-energy hadronic physics.[7] We will restrict ourselves to a one-loop approximation: $\mathcal{L}_{eff} \simeq \mathcal{L}_0 + \mathcal{L}_{\text{1-loop}}$. Here $\mathcal{L}_{\text{1-loop}}$ contains the operators that generate the one-loop proper diagrams, and vacuum polarization graphs such as Fig. 1 can then be summed to all orders via Dyson's equation,[5] yielding the full, or "dressed," photon propagator. The resulting matrix elements are all expressed in terms of bare parameters; in a renormalizable theory, however, these will never appear alone, but only in certain characteristic combinations that are finite, RS–independent, and thus physical.

We return to the example of QED. The QED Lagrangian contains one parameter, the bare electromagnetic coupling e_0. (We ignore particle masses.) Since only the transverse degrees of freedom of the photon are important in QED, we drop the tensor indices. Schematically, we write the matrix element in either the s or the t channel for the interaction of charges Q and Q':

$$M_{QED} = e_0^2 \frac{QQ'}{q^2} \tag{2.1}$$

at tree level. Introduce the proper photon self-energy, or vacuum polarization, $\Pi_{AA}(q^2)$. Then:

$$\begin{aligned} \Pi_{AA}(q^2) &= q^2\, \Pi'_{AA}(q^2) \quad , \\ \Pi_{AA}(q^2) &= e_0^2\, \Pi_{QQ}(q^2) = e_0^2\, q^2\, \Pi'_{QQ}(q^2) \quad . \end{aligned} \tag{2.2}$$

That $\Pi_{AA}(q^2)$ is proportional to q^2 is ensured by a QED Ward identity and simply means that the photon remain massless in the presence of quantum corrections. Π'_{QQ} is convenient because, to one loop, all factors of e_0 have been removed. Π'_{QQ} is dimensionless and logarithmically divergent. Using Dyson's equation,[5] we can sum the proper vacuum polarization to all orders:

$$M_{QED} = \left[\frac{e_0^2}{q^2} + \frac{e_0^2}{q^2}\,(e_0^2\,\Pi'_{QQ}) + \ldots\right] QQ'$$
$$= \frac{e_0^2\,QQ'}{q^2[1 - e_0^2\,\Pi'_{QQ}(q^2)]} \quad . \tag{2.3}$$

(We ignore the imaginary part of Π_{AA} for the moment.) e_0^2 is, of course, unmeasurable because of the radiative correction Π'_{QQ}. A concise, RS–independent way of writing the matrix element is to introduce:

$$\frac{1}{e_*^2} = \frac{1}{e_0^2} - \Pi'_{QQ}\,(q^2) \quad . \tag{2.4}$$

Then

$$M_{QED} = \frac{e_*^2\,(q^2)\;QQ'}{q^2} \quad . \tag{2.5}$$

We now define $e_*^2(q^2)$ by one experimental input, the value of e_*^2 at some q^2, replacing the free bare parameter e_0^2. This choice is the equivalent in our approach to a RS. The function e_*^2 is then well-defined and finite; it is also RS–invariant, as it is expressible in terms of bare quantities. $e_*^2(q^2)$ can be run to any q^2, circumventing the usual asymptotic RNG approximations, because $\Pi'_{QQ}(q^2)$ can be computed in closed form to any finite order using standard loop integrals.[8,9] [In this paper we compute the proper self-energies explicitly to one loop only, but the definition of $e_*^2(q^2)$ holds in general.] The Feynman rules are generated by the one-loop effective Lagrangian:

$$\mathcal{L}_{eff} = -\frac{1}{4}\,F^{\circ}_{\mu\nu}\,F^{\circ}_{\mu\nu}\,[1 - e_0^2\,\Pi'_{QQ}] + \bar{\psi}_0\left[\not{\partial} + m_0 + \begin{matrix}\text{electron}\\ \text{self-energy}\end{matrix}\right]\psi_0 \quad ,$$
$$+ ie_0\,Q\bar{\psi}_0\,\not{A}_0\,[1 + \text{vertices}]\;\psi_0 + \bar{\psi}_0\psi_0\,[\text{boxes}]\;\bar{\psi}_0\psi_0 \quad . \tag{2.6}$$

In the counterterm approach to renormalization, $\mathcal{L}_{eff}$ would be divided into two parts, $\mathcal{L}_{eff} = \mathcal{L}_{ren} + \mathcal{L}_{radcorr}$. Then $\mathcal{L}_{ren}$ would be expressed in terms

of "renormalized" parameters, based on a particular RS, with the renormalized parameters expressed as certain combinations of bare parameters and infinite parts of the one-loop corrections. The finite remainder of the one-loop terms then constitute what are usually called "radiative corrections." The division of $\mathcal{L}_{eff}$ into $\mathcal{L}_{ren} + \mathcal{L}_{rad\,corr}$, like the division of $\mathcal{L}_0$ into $\mathcal{L}_{ren} + \mathcal{L}_{ct}$, is strictly conventional, however, and without physical meaning. The alternate approach outlined here has the virtue of simplicity: the entire apparatus of renormalization schemes and counterterms is never introduced, because it is not needed.

The one-loop Lagrangian used at "tree level," so to speak, gives the one-loop corrections; using Dyson's equation, we can then sum the one-loop oblique corrections to all orders. Because we use the Dyson's equations to sum the proper oblique corrections, the correct diagrammatic expansion of $\mathcal{L}_{eff}$ is through *proper,* or *one-particle irreducible* (1PI), graphs. While we are still computing corrections perturbatively and must cut off the calculation somewhere, truncating the calculation to one loop in the irreducible diagrams forms a closed, self-consistent approximation. On the other hand, RS–dependence generally appears in matrix elements because the infinite sum [in Eq. (2.3)] has been truncated at some order. Changing from one RS to another, in general, induces errors of order higher than that retained in the matrix element; but renormalization schemes (especially in electroweak physics) are often defined in a way that implicitly includes those higher orders, even though they are absent from the matrix element. Starting from the bare Lagrangian and proceeding with the effective Lagrangian and the full Dyson's equations, such difficulties are never encountered. The one-loop $\mathcal{L}_{eff}$ can also be used, as a "tree-level" Lagrangian, as the basis for loop calculations; one then generates higher-order irreducible diagrams. In particular, the function $e_*^2(q^2)$ will now have higher-order proper diagrams in $\Pi'_{QQ}(q^2)$ (e.g., Fig. 3). The finiteness of $e_*^2(q^2)$ is then shown inductively, beginning with the simple one-loop divergences.[5] The behavior of arbitrarily complex loop diagrams is governed by Weinberg's theorem[10] In particular, e_*^2 appears in diagrams other than oblique ones (like boxes, for example, see Fig. 4) because

the full photon propagator (not the tree-level one) is inserted. The loop integrand is now convoluted with $e_*^2(q^2)$ and, in general, is quite complicated. One can develop reasonable approximations to these convolutions by determining the dominant region(s) of integration and setting $e_*^2(q^2)$ equal to its value(s) there. In this way, the RS–independent parametrization can be used in all parts of a matrix element. Finiteness and RS–invariance are evident at every step, and the matrix element takes an especially simple form. The gain in QED from this method is mainly notational, as QED is a simple theory. In a complex broken non–Abelian gauge theory like SU(2) $\times$ U(1), the introduction of the effective Lagrangian and "starred" functions will present a more striking simplification.

3. Effective Lagrangian and Radiative Corrections for Glashow–Salam–Weinberg Model

To reformulate the Glashow–Salam–Weinberg (GSW) electroweak model,[11] we need to begin with the bare Lagrangian and sum the proper self-energies in the matrix elements to all orders using Dyson's equations. This will allow us to introduce a set of "starred" functions like e_*^2. An effective Lagrangian will summarize the physics of the theory to one loop and can be manipulated like a tree-level Lagrangian, a fact that will prove useful. We will continue to calculate the gauge boson self-energies explicitly to one loop, but the procedure can be generalized to any order.

The four-fermion process $f\bar{f} \to f'\bar{f}'$ (Fig. 5) illustrates the method, and matrix elements in different channels can be obtained by crossing symmetry.[2] The complete formulation of the neutral- and charged-current matrix elements in the case of light external fermions is presented in Appendix A. (This treatment can easily be extended to massive external fermions.) The standard model of electroweak interactions requires a large set of parameters for its definition. Ignoring fermion and Higgs masses and concentrating on the gauge sector of the theory narrows the set down to three parameters (or four if there is an extended Higgs sector). In the original Lagrangian, they are the bare gauge couplings, g_0 [SU(2)] and g_0' [U(1)], and bare Higgs doublet expectation value, $\langle\phi\rangle_0$, which sets the scale for the gauge boson masses. Then one can define the sine and cosine of the weak mixing angle:

$$s_0^2 = \frac{g'^2{}_0}{g_0^2 + g'^2{}_0} \quad , \quad c_0^2 = 1 - s_0^2 \quad , \quad e_0^2 = g_0^2\, s_0^2 \quad . \tag{3.1}$$

The bare W and Z masses are then:

$$\begin{aligned} M_{W_0}^2 &= \frac{1}{2}\, g_0^2\, \langle\phi\rangle_0^2 \\ M_{Z_0}^2 &= \frac{1}{2}\, g_0^2\, \langle\phi\rangle_0^2 / c_0^2 \quad . \end{aligned} \tag{3.2}$$

Of course, none of these parameters is measurable; they are all modified by the presence of radiative corrections. Exactly as in QED, one can introduce a RS-independent and finite running parameter for each independent bare parameter. (This is why the theory is renormalizable.) We need one dimensionful quantity characterizing the Higgs doublet v.e.v. $\langle\phi\rangle_0$, which for convenience we choose to be G_{μ_0}, the bare Fermi coupling as measured by muon decay:

$$\frac{G_{\mu_0}}{\sqrt{2}} = \frac{g_0^2}{8M_{W_0}^2} \quad . \tag{3.3}$$

Our three running parameters, defined in Appendix A, are then: $e_*^2(q^2)$, $s_*^2(q^2)$ and $G_{\mu_*}(q^2)$, corresponding to e_0^2, s_0^2 and G_{μ_0}, respectively. We also introduce two auxiliary "starred" functions: $c_*^2(q^2) = 1 - s_*^2(q^2)$ and $\rho_*(q^2)$. The bare ρ parameter is conventionally defined as:

$$\rho_0 = \frac{M_{W_0}^2}{M_{Z_0}^2\, c_0^2} \quad . \tag{3.4a}$$

$\rho_0 = 1$ in the standard model, with one Higgs doublet v.e.v.. Nevertheless, $\rho_*(q^2) \neq 1$ because of radiative corrections. However, $e_*^2(q^2)$, $s_*^2(q^2)$ and $G_{\mu_*}(q^2)$ are *free* parameters in GSW, as $e_*^2(q^2)$ was in QED: we need an arbitrary experimental input at some q^2 to define them. $\rho_*(q^2)$ is not arbitrary, but *computable*, given $e_*^2(q^2)$, $s_*^2(q^2)$, $G_{\mu_*}(q^2)$ (and the fermion and Higgs masses): no independent empirical datum is necessary to fix it. If we extend the standard model to include an arbitrary number of Higgs multiplets with arbitrary isospins, ρ_0 is no longer equal to unity; it becomes a free parameter. (Equivalently, M_{W_0} and M_{Z_0} are no longer defined by Eq. 3.2.)

$$\rho_0 = 1 + \frac{\sum_{\text{all }\phi} \langle \phi_0^+ \left(\vec{I}^{\,2} - 3\, I_3^2 \right) \phi_0 \rangle_{\text{vacuum}}}{2 \sum_{\text{all }\phi} \langle\, \phi_0\, I_3^2\, \phi_0 \,\rangle_{\text{vacuum}}} \quad . \tag{3.4b}$$

$\rho_0 = 1$ can be guaranteed without fine-tuning by choosing only doublet v.e.v.'s. If other types of multiplets are used, $\rho_*(q^2)$ is no longer computable without

an independent measurement at some q^2. The general case of arbitrary Higgs structure is treated in Appendix A; in the main text, we will consider only the standard model with $\rho_0 = 1$.

The oblique, or gauge propagator, corrections (Fig. 1) can be summed up using Dyson's equations (Figs. 6 and 7). Introduce the photon, Z and $W^{\pm}$ currents:

$$\begin{aligned} J_A &= e_0\, J_Q \\ J_Z &= \frac{e_0}{s_0\, c_0}\,[J_3 - s_0^2\, J_Q] \\ J_{\pm} &= \frac{e_0}{s_0}\,\frac{[J_1 \pm i\, J_2]}{\sqrt{2}} \quad , \end{aligned} \tag{3.5}$$

and the reduced proper photon, Z–A mixing, Z and W self-energies:

$$\begin{aligned} &\Pi_{AA} = e_0^2\, \Pi_{QQ} \quad , \quad \Pi_{ZA} = \frac{e_0^2}{s_0\, c_0}\,[\Pi_{3Q} - s_0^2\, \Pi_{QQ}] \quad , \\ &\Pi_{ZZ} = \frac{e_0^2}{s_0^2\, c_0^2}\,[\Pi_{33} - 2s_0^2\, \Pi_{3Q} + s_0^4\, \Pi_{QQ}] \quad , \quad \Pi_{WW} = \frac{e_0^2}{s_0^2}\,\Pi_{11} \quad . \end{aligned} \tag{3.6}$$

To one loop, Π_{QQ}, Π_{3Q}, Π_{33} and Π_{11} have no couplings embedded in them. The Dyson's equations can be generated by the one-loop effective Lagrangian. Schematically:

$$\begin{aligned} L_{eff} = &-\frac{1}{4}\,(\text{gauge})^0_{\mu\nu}\,(\text{gauge})^0_{\mu\nu}\,[1 - \Pi\text{'s}] + [M^2_{\text{gauge}} - \Pi\text{'s}]\,(\text{vector})^2_{\mu_0} \\ &+ \overline{\psi}_0\,[\not{\partial} + m_0 + \text{fermion self-energies}]\psi_0 \\ &+ i\,\overline{\psi}_0\,(\text{vector})^{\mu}_0\,\gamma_\mu\,[1 + \text{vertices}]\,\psi_0 + \overline{\psi}_0\,\psi_0\,[\text{boxes}]\,\overline{\psi}_0\,\psi_0 \quad . \end{aligned} \tag{3.7}$$

As explained in detail in Appendix A, part of the self-energy function Π_{3Q} (Fig. 9) creates a self-inconsistency in the electroweak matrix elements, attributable to the presence in the one-loop L_{eff} of a new effective mass term mixing the Z and the photon. Related to this problem is the fact that the gauge boson self-energies due the gauge bosons themselves are not gauge-invariant, but in fact must be combined with a certain universal part of the vertices (Fig. 8). The cure

for this difficulty is to rediagonalize the neutral current sector in the one-loop Lagrangian. This is a purely non–Abelian effect having no analogue in QED. The equivalent in counterterm renormalization is a Ward identity relating part of the vertex counterterms to part of the counterterm of Π_{3Q}, but this is RS–dependent, of course.[2,9] The remaining direct corrections (bremsstrahlung, boxes and the residual vertices, with the aforementioned universal part removed) form a gauge-invariant and finite set by themselves and can be considered separately. They are also specific to the external fermions and the experimental situation; the oblique plus non–Abelian vertex parts presented here are universal to all processes mediated by electroweak vector bosons. Let I_3 and Q be the initial weak isospin and electric charge, I_3' and Q' the final; let I_+ and I_- be the charge-raising and -lowering operators, respectively. We then show in Appendix A that, apart from small but nontrivial imaginary parts, the neutral- and charged-current matrix elements are:

$$M_{NC} = \frac{e_*^2\, Q\, Q'}{q^2[1 - i\ \mathrm{Im}\Pi'^*_{AA}]} + \left(\frac{e_*^2}{s_*^2 c_*^2}\right) \frac{[I_3 - (s_*^2 - is_*\ c_*\ \mathrm{Im}\ \Pi'^*_{ZA})Q]\ [I_3' - (s_*^2 - is_*\ c_*\ \mathrm{Im}\ \Pi'^*_{ZA})Q']}{q^2 + \frac{e_*^2}{s_*^2\ c_*^2} \frac{1}{4\sqrt{2}\ G_{\mu *}\rho_*} - is\left(\frac{\Gamma_{Z*}}{\sqrt{s}}\right)} \tag{3.8}$$

and

$$M_{CC} = \frac{e_*^2}{2s_*^2} \frac{\langle I_+\ I_-\rangle}{q^2 + \frac{e_*^2}{s_*^2}\ \frac{1}{4\sqrt{2}\ G_{\mu *}} - is\ \left(\frac{\Gamma_{W*}}{\sqrt{s}}\right)}\ , \tag{3.9}$$

in either the s or t channel. The reduced proper self-energies defined in Eq. 3.6 are computed to one loop in the standard model in Appendix B. The widths are discussed in Appendix C. Equations 3.8 and 3.9 and Appendix A summarize the key results. They express the corrected four-fermion process in a finite, RS–independent way based on an effective Lagrangian and the summed Dyson's equations. The representations 3.8 and 3.9 have the additional advantage of simplicity and greater numerical accuracy, the latter another benefit of retaining the full Dyson's equations. Note that:

$$M_{Z_0}^2 = \frac{e_0^2}{s_0^2\, c_0^2} \frac{1}{4\sqrt{2}\, G_{\mu_0}\, \rho_0}$$
$$M_{W_0}^2 = \frac{e_0^2}{s_0^2} \frac{1}{4\sqrt{2}\, G_{\mu_0}} \quad . \tag{3.10}$$

One simply gets 3.8 and 3.9 by "starring" everything. The physics of the largest subset of radiative corrections has been absorbed into the running couplings. This *universality* of the starred gauge couplings is not a notational gimmick, but a consequence of the underlying gauge symmetry. The *same* e_*^2, s_*^2 and c_*^2 occur everywhere in the two matrix elements. At $q^2 = 0$, for example, the gauge factors common to the numerators and denominators of 3.8 and 3.9 cancel; similarly, at the Z and W resonance poles, the same numerator factor will cancel with identical factors in the width. (See Appendix C.) Finally, this universality is embodied in the uniqueness of the relationship between each self-energy function and its corresponding starred function. The starred functions themselves render this relationship transparent, while the counterterm approach obscures it. Such transparency is a powerful check on the consistency of the radiatively-corrected matrix elements.

To complete the theory, we must fix the value of the three independent starred functions at any q^2 (or set of q^2's); the equations of Appendix A allow us to run the functions to any other energies. Radiative corrections are now freed from the baggage of specifying a fixed set of parameters. Instead of defining a $\sin^2\theta_W$ by an experiment and speaking of radiative corrections to it in other experiments, one simply refers to the universal function $s_*^2(q^2)$ at different q^2, and so on for all the different electroweak parameters. Because the starred functions are defined in terms of the exact self-energies in 3.6, one can compute their running for any q^2 without introducing any approximations (beyond the perturbative one), in contrast to the usual RNG treatment. Comparison of electroweak experiments at different energies is now straightforward. Since the forms 3.8 and 3.9 are RS–invariant, the matrix element can be used to relate different renormalization

schemes. The scheme of Sirlin and Marciano,[12] for example, uses a weak mixing angle defined by the ratio of the W and Z masses: $\sin^2\theta_W = 1 - M_W^2/M_Z^2$. M_Z and M_W are given exactly by the poles of 3.8 and 3.9, respectively:

$$\frac{M_W^2}{M_Z^2} = \left[\frac{e_*^2}{s_*^2}\,\frac{1}{G_{\mu *}}\right]_{q^2=-\,M_W^2} \left[\frac{e_*^2}{s_*^2\,c_*^2}\,\frac{1}{G_{\mu *}\rho_*}\right]^{-1}_{q^2=-\,M_Z^2} \quad . \tag{3.11}$$

By approximating that the starred functions run very little between the W and Z poles, we get to tolerable accuracy:

$$\sin^2\theta_W = s_*^2(Z) - (\rho_*(Z) - 1)\; c_*^2(Z) \quad . \tag{3.12}$$

[See, however, Section 6, Eqs. (6.2a) and (6.2b).] The scheme used in this paper, that of Lynn, Peskin and Stuart,[2] uses α, G_μ, and M_Z, the pole of 3.8, as inputs in defining the starred functions. One can now compute M_W, for example. The results of one scheme become the starting point for another and the mutual consistency of different schemes is assured.

As the Z and W propagators no longer have simple Breit–Wigner forms, the interpretation of the resonance shapes becomes somewhat subtle. In particular, the resonance shape is changed to:

$$\frac{1}{(q^2 + M^2)(1+\kappa) - i\; s\; \left(\frac{\Gamma_*}{\sqrt{s}}\right)} \quad . \tag{3.13}$$

Besides the phase space factor s and the radiative corrections in Γ_*, the additional $1+\kappa$ changes the interpretation of the experimental width. The resonance pole structure and its effect on the line shape are taken up in detail in Appendix C.

4. Running of Renormalization Scheme–Independent Parameters in SU(2) × U(1)

We use the scheme of Ref. 2, as mentioned. α and G_μ are already known to high accuracy, leaving as unknown parameters of the standard model the Z mass (M_Z), the top quark mass (m_t) and the Higgs mass (m_H). In this section we illustrate some of the behavior of the running starred functions. The results presented should be taken as accurate predictions for the standard GSW model to one loop with three generations of quarks and leptons. In this paper, and in related Monte Carlo simulations (to be published shortly),[13] we have used a simple analytic dispersion relation for the low-energy hadronic contribution to Π_{QQ} and related it to the analogous contribution to Π_{3Q} by manipulation of the fundamental currents and ignoring the mixings of the different vector hadrons, as outlined in the paper of Lynn, Penso and Verzegnassi.[14] This retains all the necessary hadronic corrections to the Π's, except for terms suppressed by powers of small quark masses. Heavy quark contributions to the Π's are computed perturbatively, with QCD corrections added to the imaginary (but not the real) parts.[2] Our results substantially confirm those of Ref. 2, while (1) improving their numerical accuracy and allowing a much larger top mass, and (2) considerably simplifying the conceptual organization of radiative corrections.

The gauge boson self-energies Π have a general structure that allows for a neat separation of various physical effects. The Π's are expressible in terms of the standardized dimensionless form factors of Passarino and Veltman.[8] However, the self-energies have canonical dimension of (energy)^2 and so must have some dimensioned factor multiplying the form factors. This factor is either q^2, the invariant mass-squared of the virtual gauge boson, or is the square of a mass of a particle circulating in the loop diagram. We call a Π proportional to q^2 "transverse," and a Π proportional to a (mass)^2 "longitudinal." In an unbroken gauge theory, all the Π's are strictly transverse, as there are only *transverse* gauge degrees of freedom, and they renormalize the gauge couplings, as in QED.

The presence of longitudinal Π's is allowed only because of symmetry-breaking, corresponding to the presence of real gauge boson masses and of *longitudinal* gauge degrees of freedom, and these longitudinal parts renormalize the vacuum expectation values responsible for the vector boson masses. (Hence the names; note, however, that this usage of "transverse" and "longitudinal" self-energies differs from, but is related to, their usual meanings.) The transverse part of a Π will be denoted by Π^T, and

$$\Pi^T \equiv q^2 \Pi' \quad , \tag{4.1}$$

as in Section 2. A longitudinal part will be written as Π^L:

$$\Pi \equiv \Pi^T + \Pi^L = q^2 \Pi' + \Pi^L \quad .$$

Consult Appendix B for a discussion of the general structure of the loop integrals and their behavior in various regimes.

Now Π_{QQ} and a gauge-invariant combination of Π_{3Q} and a non–Abelian vertex function Γ' are purely transverse and renormalize the gauge couplings. Π_{33} and Π_{11} have both transverse and longitudinal parts. The longitudinal parts, being proportional to the squares of masses, are sensitive to heavy particles, a topic to be taken up in the next section and in a subsequent paper.[15] $e^2 = e_*^2(0) = 4\pi\alpha$. Then:

$$\begin{aligned} e_*^2(q^2) &= \frac{e^2}{1 - e^2 \Delta_Q(q^2)} \quad , \\ \Delta_Q(q^2) &= \mathrm{Re}\left[\Pi'_{QQ}(q^2) + 2\Gamma'(q^2) - \Pi'_{QQ}(0) - 2\Gamma'(0)\right] \quad , \end{aligned} \tag{4.3}$$

just as in Section 2, with the addition of the vertex function Γ' needed in the non–Abelian theory. Figure 11 illustrates the running of $4\pi/e_*^2(q^2)$ from 1 MeV to 1 TeV (q^2 timelike and spacelike). We have used $M_Z = 93$ GeV, $m_t = 40$ GeV and $m_H = 100$ GeV. The fermions make e_*^2 run faster (noticeable as we pass into the GeV region), while the well-known non–Abelian nature of the W's slows the running down, contributing to Δ_Q with a sign opposite from that of the fermions

(the W^+W^- threshold is about 160 GeV). The asymptotic behavior of e_*^2 is of course logarithmic, as given by the renormalization group:

$$\begin{aligned} e_*^2(q^2) &= \frac{e^2(\mu^2)}{1 - e^2(\mu^2)\,\beta\,\ell n\left(\frac{q^2}{\mu^2}\right)} \quad , \\ \beta &= \frac{-1}{48\pi^2}\left[11N - \frac{32N_g}{2} - 1\right] \quad , \end{aligned} \tag{4.4}$$

where N_g is the number of fermion generations in the theory and $N = 2$ for SU(2); μ^2, $q^2 \gg$ (masses)^2. The three contributions to β are from the vector, fermion and scalar particles, respectively. In Fig. 12 we show $s_*^2(q^2)$ over the same energy range, with the same masses. Its behavior can best be understood if we define a running SU(2) coupling $g_*^2 = e_*^2/s_*^2$. Then

$$\frac{1}{g_*^2(q^2)} - \frac{1}{g_*^2(\mu^2)} = -\mathrm{Re}\left[\Pi'_{3Q}(q^2) + 2\Gamma'(q^2) - \Pi'_{3Q}(\mu^2) - 2\Gamma'(\mu^2)\right] \quad , \tag{4.5}$$

apart from some small corrections. Until the W^+W^- threshold, both $e_*^2(q^2)$ and $g_*^2(q^2)$ increase with the fermionic logarithms, but $g_*^2(q^2)$ runs up faster—hence, $s_*^2(q^2)$ decreases. Once the $2W$ threshold is passed, $g_*^2(q^2)$ behaves like a true non–Abelian coupling and decreases. (The difference between the timelike and spacelike graphs of Fig. 12 is due to the different W threshold behavior in the two regions.) $s_*^2(q^2)$ henceforth increases asymptotically in the usual RNG manner to its SU(5) GUT value of 3/8, somewhere between[16] 10^{14} and 10^{15}. Asymptotically:

$$\begin{aligned} g_*^2(q^2) &= \frac{g^2(\mu^2)}{1 - g^2(\mu^2)\,\beta'\,\ell n\left(\frac{q^2}{\mu^2}\right)} \quad , \\ \beta' &= \frac{1}{48\pi^2}\left[11N - 4N_g - \frac{1}{2}\right] \quad . \end{aligned} \tag{4.6}$$

In our RS, M_Z is an input parameter; thus, $s_*^2(Z)$ is the renormalization point for defining $s_*^2(q^2)$ [or $g_*^2(q^2)$] in Eq. (4.5):

$$s_*^2(Z)\,c_*^2(Z) \;=\; \frac{1}{M_Z^2}\,\frac{e_*^2(Z)}{4\sqrt{2}\,G_{\mu_*}(Z)\,\rho_*(Z)} \quad , \tag{4.7}$$

where $c_*^2 = 1 - s_*^2$. In keeping with the Appelquist–Carazzone theorem,[17] heavy particles decouple from the *running* (the slopes) of $e_*^2(q^2)$ and s_*^2 (controlled by Π'_{QQ} and Π'_{3Q}); however, s_*^2, unlike e_*^2, is normalized by its value at the Z° pole and is affected by G_{μ_*} and ρ_*, functions which are *quite sensitive* to the effects of heavy particles. Broken gauge theories generally exhibit a nondecoupling of heavy particles at low energies, a subject to which we now turn our attention.

5. Heavy Physics in the Standard Model—General Classification of Effects

As a general rule, one expects heavy particles to decouple at energies much lower than their masses.[17] For example, the low-energy world of unbroken SU(2) × U(1) is protected from the effects of heavy gauge bosons whose masses are due to large v.e.v.'s; corrections from the heavy bosons are suppressed by inverse powers of their mass. In theories with broken global and local symmetries, however, decoupling in radiative corrections no longer holds if masses become large through the increase of a dimensionless parameter (e.g., Yukawa, gauge or scalar self-couplings).[18] (This is quite apart from effects in scalar masses such as the gauge hierarchy problem.) The standard electroweak model thus becomes a laboratory for the detection of heavy particles. Nondecoupling has been examined by a number of authors.[2,9,19,20,21,22] The starred functions allow a simple and general scheme for classifying these effects.

Clearly, heavy physics makes its presence known through the longitudinal parts of the oblique corrections, since they are proportional to the squares of masses. $G_{\mu_*}(q^2)$ and $\rho(q^2)$ are the two functions whose behavior is controlled by the longitudinal parts. G_μ is the measured muon decay constant (but see Appendix A):

$$G_{\mu_*}(q^2) = \frac{G_\mu}{1 - 4\sqrt{2}\, G_\mu\, \Delta_1(q^2)} \quad , \tag{5.1}$$

$$\Delta_1(q^2) = \mathrm{Re}\left\{\Pi_{11}(q^2) - \Pi_{3Q}^T(q^2) - \Pi_{11}(0) - 2M_W^2\left[\Pi_{3Q}^L(q^2) - \Pi_{3Q}^L(0)\right]\right\} \; ;$$

$$\rho_*(q^2) = \frac{1}{1 - 4\sqrt{2}\, G_{\mu_*}\, \Delta_\rho(q^2)} \quad , \tag{5.2}$$

$$\Delta_\rho(q^2) = \mathrm{Re}\left[\Pi_{33}(q^2) - \Pi_{11}(q^2)\right] \quad .$$

Note we can define:

$$\Delta_3(q^2) \;=\; \mathrm{Re}\left\{\Pi_{33}(q^2) - \Pi_{3Q}^T(q^2) - \Pi_{33}(0) - 2M_W^2\left[\Pi_{3Q}^L(q^2) - \Pi_{3Q}^L(0)\right]\right\} \quad , \tag{5.3}$$

in analogy with $\Delta_1(q^2)$. Then,

$$\Delta_3(q^2) - \Delta_1(q^2) \;=\; \Delta_\rho(q^2) - \Delta_\rho(0) \quad . \tag{5.4}$$

The best-known heavy particle effects come from isospin splittings in multiplets; these are measured by $\Delta_\rho(q^2)$. At $q^2 = 0$, ρ_* becomes the conventional radiatively-corrected ρ–parameter,[22] with the corrections summed:

$$\rho_* \;=\; \frac{1}{1 - \delta\rho_*} \quad . \tag{5.5}$$

The scale in $\delta\rho_*$ is set by $G_\mu \simeq [2\sqrt{2}\,\langle\phi\rangle^2]^{-1}$. Hence, isospin splittings need to become of order $\langle\phi\rangle$ before they appreciably correct ρ_*. In the fermionic sector in the standard model with three generations, the only hope of such large splittings is in the top-bottom doublet. If $m_t^2 \gg m_b^2$, then the contribution to $\delta\rho_*$ diverges quadratically, a well-known result:[22]

$$\begin{aligned} \delta\rho_*(0) \;&=\; \frac{3G_\mu}{8\sqrt{2}\,\pi^2}\left[m_t^2 + m_b^2 - \frac{2m_t^2 m_b^2}{m_t^2 - m_b^2}\,\ell n\,\left(\frac{m_t^2}{m_b^2}\right)\right] \quad , \\ &\xrightarrow[m_t \gg m_b]{} \frac{3G_\mu m_t^2}{8\sqrt{2}\,\pi^2} \quad , \qquad \xrightarrow[m_t = m_b]{} 0 \quad . \end{aligned} \tag{5.6}$$

We illustrate $\rho_*(0)$ as a function of m_t, with $M_Z = 93$ GeV and $m_H = 100$ in Fig. 13, which shows the quadratic divergence of Eq. (5.6) with m_t in a dramatic fashion. The isospin splitting (due to hypercharge) between the Z and the W also makes $\rho_*(0)$ dependent on the Higgs mass m_H, but only very weakly:

$$\delta\rho_*(0) = \frac{3G_\mu}{8\sqrt{2}\pi^2}\left[M_W^2\,\ell n\left(\frac{m_H^2}{M_W^2}\right) - M_Z^2\,\ell n\left(\frac{m_H^2}{M_W^2}\right)\right] \quad , \qquad (5.7)$$
$$m_H \gg M_W, M_Z \quad .$$

Figure 14 shows the slow decrease in $\rho_*(0)$ with m_H. Note that $\rho_*(0)$ decreases as long as $M_W < M_Z$. A gauge boson contribution to $\delta\rho_*(0)$ has the opposite sign of 5.6, a fermionic contribution. However, the indirect effect of a large top mass is to increase M_W strongly. For $m_t = 1000$ GeV, $M_W > M_Z$, so that $\rho_*(0)$ now *increases* with m_H (see Table I). Note:

$$\Delta_\rho(q^2) = q^2\left(\Pi'_{33} - \Pi'_{11}\right) + \Pi^L_{33} - \Pi^L_{11} \quad . \qquad (5.8)$$

As q^2 increases towards the weak scale, the transverse parts increase at first; once all the mass thresholds are passed, however, the asymptotic (logarithmic) behavior of Π'_{33}, Π'_{11}, Π^L_{33} and Π^L_{11} sets in and all the isospin splittings cancel, leaving us with the general result: $\Delta_\rho(q^2 \to \infty) = 0$. This illustrates a general property of the starred functions: *as $q^2 \to \infty$, they approach the value of the corresponding bare parameter.* The running of $\rho_*(q^2)$ is shown for various top masses in Fig. 15 (also Table II). $\rho_*(0)$ is sensitive to any kind of isospin splittings, in particular from new generations of fermions or scalars and, on the basis of νN scattering, already been used to set an upper bound of several hundred GeV on the mass splittings of particles[23] coupled to the Z and W.

Heavy physics is also detectable in the independent function $\Delta_1(q^2)$ or, equivalently, Δ_3 [because of Eq. (5.3)]. Unlike $\Delta_\rho(q^2)$, however, Δ_3 is sensitive to *degenerate* fermions.[2] We illustrate this in Fig. 16 with $G_{\mu_*}(Z)$ ($M_Z =$ 93 GeV and $m_H = 100$ GeV), where the top and bottom quark masses have been set equal and the common mass is allowed to vary over 1 TeV. If

$$G_{\mu_*} = \frac{G_\mu}{1 - \delta G_{\mu_*}} \quad , \qquad (5.9)$$

then the shift δG_{μ_*} from a heavy degenerate pair of fermions at the Z pole is

$$\delta G_{\mu\bullet}(Z) \;=\; -\frac{3M_Z^2\,G_\mu}{12\sqrt{2}\,\pi^2} \quad , \qquad m_t = m_b \;\gg\; M_Z \quad . \tag{5.10}$$

This effect comes directly from the longitudinal part. For a fixed q^2 (e.g., $-M_Z^2$), the longitudinal part becomes independent of the heavy mass m for $|q^2| \ll m^2$:

$$\Pi^L(q^2) - \Pi^L(0) \;\sim\; m^2 \left(\frac{q^2}{m^2}\right) \quad . \tag{5.11}$$

Degenerate fermion masses do not break global isospin symmetry and hence do not contribute to Δ_ρ, but their presence signals the breaking of the global chiral symmetry of the Glashow–Salam–Weinberg (GSW) theory. Note that this means that heavy degenerate scalars are not detectable. In Table III and Fig. 17, we show how $G_{\mu\bullet}(Z)$ varies with m_t and m_H (m_b has been set to its normal value). As m_t becomes large, $G_{\mu\bullet}(Z)$ becomes constant [Eq. (5.8)]; but as m_t goes to 1 TeV, the indirect effect of the large W mass pushes $G_{\mu\bullet}(Z)$ back up. Shifts in Δ_1 (or Δ_3), since they are small constants, compete with the quadratically-diverging Δ_ρ; if the latter is large enough, Δ_1 and Δ_3 are swamped. Figure 18 shows the running of $G_{\mu\bullet}(q^2)$. The asymptotic behavior is controlled by:

$$32\pi^2\Delta_1(q^2 \to \infty) = \left[3\sum_q m_q^2 + \sum_\ell m_\ell^2 + \frac{1}{4}\,m_H^2 - \frac{1}{2}\,\left(10m_W^2 + 3M_Z^2\right)\right] \ell n(q^2)\,, \tag{5.12}$$

where "q" is all quarks and "ℓ" all leptons.

If the fermion and Higgs masses grow very large (on the order of a few TeV), the perturbation theory breaks down. These masses are proportional to dimensionless couplings, Yukawa couplings in one case and the scalar self-coupling in the other. Generally, the perturbation theory ceases to be valid when these couplings are of order unity; however, in this context, the expansion parameter in radiative corrections is of the form $G^2/16\pi^2$ (where G is a dimensionless coupling), so we expect breakdown when $G \sim 4\pi$. This corresponds to fermion

masses between 2 and 3 TeV. In this case, nonperturbative techniques, modeled on the chiral Lagrangians of current algebra, are available for estimating[24] the Π's. The general structure of radiative corrections given here remains valid and the reduced forms of the charge and isospin currents [Eq. (3.5)] can be directly analyzed using symmetry relations. Similar remarks can be made about some technicolor theories. In the nonperturbative case, one simply exchanges our perturbatively computable effective Lagrangian for another one based on an electroweak current algebra.

If there are nondoublet Higgs v.e.v.'s, then the function ρ_* is no longer computable without the measured value of ρ_* at some q^2 as an input. Let $\rho \equiv \rho_*(0)$ (measured in neutrino scattering, for example). Then, as shown in Appendix A:

$$\begin{aligned} \rho_*(q^2) &= \frac{\rho}{1 - 4\sqrt{2}\, G_{\mu_*}\, \rho \Delta_\rho(q^2)} \quad , \\ \Delta_\rho(q^2) &= \Delta_3(q^2) - \rho^{-1}\Delta_1(q^2) \quad . \end{aligned} \tag{5.13}$$

Now the characteristic quadratic mass divergence of isospin splittings [Eq. (5.6)] *disappears.* Any shifts from $\Delta_\rho(q^2)$, $q^2 \neq 0$, due to heavy physics, are like those in G_{μ_*}: constants independent of mass. Formally, nondoublet v.e.v.'s destroy the famous "custodial" SU(2) $\times$ SU(2) symmetry of the standard model.[7,22] Without knowing explicitly the Higgs vacuum structure, we lose a great deal of the GSW theory's predictive power.

6. Measuring Heavy Physics

The chief advantage of the methods presented in this paper is the simplicity they allow in the organization of radiative corrections. In particular, because the standard electroweak model is a broken gauge theory, the measurement of low-energy parameters can teach us about some of the heavy physics lying at energies beyond those currently accessible. This information is summarized in the functions Δ_ρ and Δ_3, and three simple observables can be used to determine them.

The first is $\rho_*(0)$, as measured in low-energy νN, νe and eD scattering. This directly gives us $\Delta_\rho(0)$ and information about isospin splittings in all multiplets coupled to the Z and the W. The second is the relationship between s_*^2 and M_*^2, Eq. (4.7). Rewriting this:

$$s_*^2(Z)\, c_*^2(Z) \;=\; \frac{e_*^2(Z)}{4\sqrt{2}\, M_Z^2\, G_\mu} \left\{1 - 4\sqrt{2}\, G_\mu \left[\Delta_3(Z) + \Delta_\rho(0)\right]\right\} . \qquad (6.1)$$

Given M_Z, $s_*^2(Z)$ measures $\Delta_3(Z) + \Delta_\rho(0)$ and, as explained below, $s_*^2(Z)$ can be measured directly in the left-right polarization asymmetry at the Z resonance. Thus $\rho_*(0)$ and $s_*^2(Z)$ determine $\Delta_\rho(0)$ and $\Delta_3(Z)$, separately. Not surprisingly, $s_*^2(Z)$ is mainly sensitive to $\Delta_\rho(0)$. In Fig. 19 and Table IV, we show the effect on $s_*^2(Z)$ of varying m_t, behavior understandable in terms of $\rho_*(0)$. The *running* of $s_*^2(q^2)$ depends only on Π'_{3Q} and is thus independent of heavy physics (except for the indirect effects of M_W). The dotted line of Fig. 19 shows $s_*^2(0)$, a quantity measurable in neutrino scattering, eD scattering and atomic parity violation experiments. The main effect of varying m_t is to shift the overall normalization of $s_*^2(q^2)$, as seen in Fig. 20 and Table V. We can also vary the Higgs mass and get a similar, but much weaker, effect (Fig. 21; see also Figs. 22 and 23). The third quantity, closely related to the first two, is M_W as computed in Eqs. (3.9) and (A.53), from the pole of the charged-current matrix element (the physical W mass). Figure 24 and Table VI show the dramatic effect, through $\Delta_\rho(0)$, that

a large top mass has on the W mass. Again, the effect of a heavy Higgs on M_W is only logarithmic (Fig. 25 and Table VII). As in Eq. (3.12), we make the approximation that the starred functions run very little between the Z and W poles, and get the approximate relationship:

$$\frac{M_W^2}{\rho_*(0)\, c_*^2(Z)\, M_Z^2} \simeq 1 \,. \tag{6.2a}$$

This relationship can directly test for the presence of a new neutral vector boson (Z'). Even at tree level, $\rho_*(0)$ and $c_*^2(Z)$ receive different corrections from the Z', depending on their experimental definition.[25] In general:

$$\frac{M_W^2}{\rho_*(0)\, c_*^2(Z)\, M_Z^2} \simeq 1 + O\left(\frac{M_Z^2}{M_{Z'}^2}\right) \,. \tag{6.2b}$$

The GSW value of this ratio is close to unity, calculable and almost completely independent of even very large radiative corrections (see Table VIII). The ratio is also essentially independent of the Higgs vacuum structure, if we assume v.e.v.'s more general than doublets.

Equation (6.2) gives us a prediction for M_W, if we know $\rho_*(0)$, $c_*^2(Z)$ and M_Z. The current accuracy[28] on $\rho_*(0)$ from neutrino scattering is about 1%, with $\rho_*(0) = 0.998 \pm 0.008$. From Eqs. (5.2) and (5.6), this is sufficient to detect isospin breakings larger than approximately 300 GeV (neglecting color and other group factors). To improve this by another order of magnitude, to tens of GeV, would require knowing $\rho_*(0)$ to one part in 10^4. An accuracy of better than 10^{-3} is perhaps more realistic and can be attained through the use of $s_*^2(Z)$, directly measurable in polarized e^+e^- experiments at the Z pole. Such an accuracy improves the isospin bound by a factor of $\sqrt{10} \sim 3$, to roughly 100 GeV. The left-right polarization asymmetry for e^+e^- beams at the Z is

$$A_{LR}(Z) \simeq \frac{-2\left[4s_*^2(Z) - 1\right]}{1 + \left[4s_*^2(Z) - 1\right]^2} \,, \tag{6.3}$$

if the photon exchange is neglected and only oblique corrections are included. The major advantage of A_{LR} is that, unlike the forward-backward asymmetry,

it is only weakly dependent on the vertex and box corrections and is essentially independent of bremsstrahlung, final state QCD and hadronization effects.[26] Thus, the hadron data of the SLC/LEP experiments can be used to measure A_{LR}, greatly improving the statistics. With hadrons, 10^6 Z events and a polarization error of 1%, A_{LR} can be measured[26] to ± 0.008. (See also Fig. 26.) Since

$$\delta A_{LR}(Z) \simeq -8\delta s_*^2(Z) \,, \tag{6.4}$$

this allows us to measure $s_*^2(Z)$ to ± 0.001. Using Eq. (6.1), we have:

$$\delta s_*^2(Z) \simeq -\frac{e_*^2(Z)}{4\sqrt{2}\, M_Z^2\, G_\mu}\, (2\delta\rho_*) \,, \tag{6.5}$$

ignoring the effect of Δ_3. This gives us isospin-splitting bounds in $\delta\rho_*$ to:

$$\sqrt{\Delta m^2} \simeq \frac{4\pi\, M_Z}{e_*(Z)} \sqrt{\frac{\delta s_*^2(Z)}{2}} = \frac{\pi\, M_Z}{e_*(Z)} \sqrt{\delta A_{LR}} \,, \tag{6.6}$$

or about 90 GeV, for $M_Z = 93$ GeV. This accuracy in A_{LR} also just brings to the surface the constant shifts in Δ_3 due to heavy degenerate fermions, such as heavy gaugings. These contribute:

$$\Delta_3(Z) \simeq \frac{-i(i+1)(2i+1)\, N_c\, M_Z^2}{144\pi^2} \,, \tag{6.7}$$

for a fermion multiplet of isospin weight i. (N_c = the number of colors: $N_c = 3$ for quarks, $N_c = 1$ for leptons.) This contributes to $\delta s_*^2(Z)$ by an amount:

$$\delta s_*^2(Z) \simeq \frac{-i(i+1)(2i+1)\, e_*^2(Z)\, N_c}{72\pi^2} \,, \tag{6.8}$$

or about $\delta s_*^2(Z) \simeq 0.0005$, or $\delta A_{LR} \simeq 0.004$, for a pair of quarks. These may be measurable in a second-generation polarization experiment. A more complete presentation of the effects of new physics on A_{LR} may be found in Ref. 2, and will be discussed is a forthcoming paper.[15]

The hierarchy of effects in the standard model suggests the following approach to checking it:

1. Verify the tree level of the standard model. Much of this has been done, but the three-gauge-boson vertex ($e^+e^- \to W^+W^-$) and the Higgs boson remain untested.

2. Test the *running* of parameters not dependent on heavy physics, i.e., e_*^2 and s_*^2.

3. Probe $\Delta_\rho(0)$ for the presence of isospin-breaking, either through $\rho_*(0)$ (neutrino scattering, atomic parity violation) or through a combination of $s_*^2(Z)$ (SLC/LEP) and M_W (LEP II). Check for a Z' through Eq. (6.2b).

4. Separate the effects of Δ_3 (or Δ_1) to look for heavy degenerate fermions.

7. Conclusions

The method of the effective Lagrangian, beginning with the bare Lagrangian and summing the radiative corrections into the running starred functions, offers a strikingly simple way of sorting out the effects of quantum corrections in the standard model. It is especially convenient for the purposes of Monte Carlo simulations, something examined in a paper to be published shortly.[13] In subsequent papers, we will consider explicit models of new physics and the constraints placed on them by low-energy measurements.[15,27] The presence of heavy physics in the next generation of electroweak experiments, although small, is measurable and emphasizes the importance and sensitivity of polarization experiments at SLC/LEP. These experiments, through the effect of radiative corrections, will inaugurate a new era in precise tests of the Glashow–Salam–Weinberg model and the high-energy world beyond it.

Acknowledgements

We would like to thank the Mark II and SLD collaborations at SLAC for their support, encouragement and criticism. We are also indebted to Robin G. Stuart for the use of his thesis (Ref. 9).

Appendix A. Effective Lagrangian, Dyson's Equations and Matrix Elements for the Standard Model

In this appendix we reformulate the four-fermion matrix elements of the Glashow–Salam–Weinberg (GSW) model to show explicitly their finiteness and RS–independence, introducing a new set of universal running couplings which are themselves RS–invariant and denoted by the subscript '$*$'. We work to one loop in the proper self-energies.

Following the spirit of Sections 2 and 3, we calculate the four-fermion neutral- and charged-current matrix elements with the effective Lagrangian, containing tree- and one-loop contributions, and sum the gauge propagator ("oblique") corrections to all orders by Dyson's equations. The effective Lagrangian will be used to analyze the neutral current sector. The method outlined here is quite general and can be applied to any process in the GSW theory and, indeed, to any gauge theory. In 't Hooft's R_ξ gauge with $\xi = 1$, we have, in general, a complicated set of Dyson's equations for the four-fermion processes.[9,28] In Fig. 6, we show the set of all neutral currents, containing the photon A, the Z and the Z's would-be Goldstone boson, ϕ_Z. (The physical Higgs decouples from this system because of CP invariance.) The system of charged currents is shown in Fig. 7, with the would-be Goldstones $\phi^\pm$ of the $W^\pm$ included. The solid circles represent the full propagators, the open ones the proper self-energies. These systems of equations drastically simplify if we use light fermions on the external legs; then the scalars ϕ_Z, $\phi^\pm$ and H (physical Higgs), and the longitudinal parts of the gauge boson propagators $\propto q_\mu q_\nu$ are suppressed, leaving only the transverse photon, Z, and $W^\pm$ propagators $\propto \delta_{\mu\nu}$, in Euclidean metric. We consider only this simplified case and omit the tensor indices. In the nomenclature of this paper, we will normally call "transverse" a self-energy proportional to q^2, and "longitudinal" a self-energy proportional to a mass-squared, following Section 4.

To keep the discussion somewhat general, we assume an arbitrary Higgs vacuum structure. The bare couplings are the SU(2) g_0 and the U(1) g_0', the bare

SU(2) fields W_0^i and the bare U(1) B_0. Then the bare weak sine, cosine, Z and photon are:

$$\begin{aligned} s_0^2 &= \frac{g_0'^2}{g_0^2 + g_0'^2} \quad , \quad c_0^2 = 1 - s_0^2 \quad , \\ Z_0 &= \left(g_0^2 + g'^2{}_0\right)^{-1/2} \left(g_0 W_0^3 - g_0' B_0\right) \quad , \\ A_0 &= \left(g_0^2 + g'^2{}_0\right)^{-1/2} \left(g_0' W_0^3 + g_0 B_0\right) \quad ; \end{aligned} \tag{A.1}$$

and the bare electric charge:

$$\frac{1}{e_0^2} = \frac{1}{g_0^2} + \frac{1}{g'^2{}_0} \quad . \tag{A.2}$$

With a Higgs multiplet of arbitrary isospin $\vec{I}$, the bare gauge boson masses are:

$$\begin{aligned} M_{W_0}^2 &= g_0^2 \left\langle \phi_0^+ \left(\vec{I}^2 - I_3^2\right) \phi_0 \right\rangle_0 \\ M_{Z_0}^2 &= 2 \left(g_0^2 + g_0'^2\right) \left\langle \phi_0^+ I_3^2 \phi_0 \right\rangle_0 \quad . \end{aligned} \tag{A.3}$$

Define the vacuum expectation values as: $\langle \ldots \rangle_0 \equiv \langle \ldots \rangle_{\text{vacuum}}$. These formulas can be easily generalized to many multiplets by simply summing the contribution of each Higgs. Conventionally, a bare ρ_0 parameter is introduced:

$$M_{W_0}^2 = \rho_0 \, C_0^2 \, M_{Z_0}^2 \tag{A.4}$$

with

$$\rho_0 = 1 + \frac{\sum_\phi \left\langle \phi_0^+ (\vec{I}^2 - 3 I_3^2) \, \phi_0 \right\rangle_0}{\sum_\phi 2 \left\langle \phi_0^+ \, I_3^2 \, \phi_0 \right\rangle_0} \quad . \tag{A.5}$$

Note that $\rho_0 = 1$ for Higgs doublets (such as in the standard model).

To set up a four-fermion matrix element, we need the full propagators G_{AA} (photon), G_{ZA} (photon–Z mixing), $G_{ZZ}(Z^0)$ and $G_{WW}(W^\pm)$. The matrix elements are:

$$\begin{aligned} \mathcal{M}_{NC} &= e_0^2\, G_{AA}\, QQ' + e_0^2 \left[Q \left(\frac{I_3' - s_0^2 Q'}{s_0 c_0} \right) + Q' \left(\frac{I_3 - s_0^2 Q}{s_0 c_0} \right) \right] G_{ZA} \\ &+ e_0^2 \left(\frac{I_3 - s_0^2 Q}{s_0 c_0} \right) \left(\frac{I_3' - s_0^2 Q'}{s_0 c_0} \right) G_{ZZ} \quad ; \\ \mathcal{M}_{CC} &= \frac{e_0^2}{2 s_0^2} \langle I_+ I_- \rangle \, G_{WW} \quad . \end{aligned} \tag{A.6}$$

Q, I_3 and Q', I_3' are the electric charge and weak (left-handed) isospin of the initial and final state fermions, respectively. I_+ and I_- are the (isospin) charge-raising and -lowering operators. We have left out the explicit vertex factors, apart from couplings and quantum numbers, because they can be treated separately (see below, however). The Dyson's equations for the G's, following Figs. 5 and 6, are:

$$\begin{aligned} G_{AA} &= D_{AA} + D_{AA}\, \Pi_{AA}\, G_{AA} + D_{AA}\, \Pi_{ZA}\, G_{ZA} \quad , \\ G_{ZZ} &= D_{ZZ} + D_{ZZ}\, \Pi_{ZZ}\, G_{ZZ} + D_{ZZ}\, \Pi_{ZA}\, G_{ZA} \quad , \\ G_{ZA} &= D_{ZZ}\, \Pi_{ZZ}\, G_{ZA} + D_{ZZ}\, \Pi_{ZA}\, G_{AA} \quad , \\ G_{WW} &= D_{WW} + D_{WW}\, \Pi_{WW}\, G_{WW} \quad . \end{aligned} \tag{A.7}$$

We have introduced the bare tree-level propagators:

$$D_{AA} = \frac{1}{q^2} \, , \qquad D_{ZZ} = \frac{1}{q^2 + M_{Z_0}^2} \, , \qquad D_{WW} = \frac{1}{q^2 + M_{W_0}^2} \quad , \tag{A.8}$$

and the proper self-energies Π_{AA}, Π_{ZA}, Π_{ZZ} and Π_{WW}, in an obvious notation. To simplify the oblique corrections, we introduce a set of reduced proper self-energies. The electroweak currents are defined as:

$$
\begin{aligned}
J_A &= e_0 J_Q \quad , \\
J_Z &= \frac{e_0}{s_0 c_0} \left(J_3 - s_0^2 J_Q \right) \quad , \\
J_\pm &= \frac{e_0}{s_0} \frac{J_1 \pm i J_2}{\sqrt{2}} \quad .
\end{aligned}
\tag{A.9}
$$

Then the proper self-energies are:

$$
\begin{aligned}
\Pi_{AA} &= e_0^2 \Pi_{QQ} \quad , \\
\Pi_{ZA} &= \frac{e_0^2}{s_0 c_0} \left(\Pi_{3Q} - s_0^2 \Pi_{QQ} \right) \quad , \\
\Pi_{ZZ} &= \frac{e_0^2}{s_0^2 c_0^2} \left(\Pi_{33} - 2 s_0^2 \Pi_{3Q} + s_0^4 \Pi_{QQ} \right) \quad , \\
\Pi_{WW} &= \frac{e_0^2}{s_0} \Pi_{11} \quad .
\end{aligned}
\tag{A.10}
$$

To one loop, Π_{QQ}, Π_{3Q}, Π_{33} and Π_{11}, have no factors of couplings embedded in them. The solution of the Dyson's equations is:

$$
\begin{aligned}
G_{AA} &= \frac{1}{q^2 - \Pi_{AA}} + \frac{\left(\frac{\Pi_{ZA}}{q^2 - \Pi_{AA}} \right)^2}{q^2 + M_{Z_0}^2 - \Pi_{ZZ} - \frac{(\Pi_{ZA})^2}{q^2 - \Pi_{AA}}} \, , \\
G_{ZA} &= \frac{\frac{\Pi_{ZA}}{q^2 - \Pi_{AA}}}{q^2 + M_{Z_0}^2 - \Pi_{ZZ} - \frac{(\Pi_{ZA})^2}{q^2 - \Pi_{AA}}} \, , \\
G_{ZZ} &= \frac{1}{q^2 + M_{Z_0}^2 - \Pi_{ZZ} - \frac{(\Pi_{ZA})^2}{q^2 - \Pi_{AA}}} \, , \\
G_{WW} &= \frac{1}{q^2 + M_{W_0}^2 - \Pi_{WW}} \quad .
\end{aligned}
\tag{A.11}
$$

We can now substitute these full propagators into the matrix elements.

A number of curious difficulties arise, however. By current conservation, the self-energy function Π_{ZA}, or, equivalently, Π_{3Q}, should be purely transverse. In the sector of loop corrections due to the gauge bosons, nevertheless, Π_{3Q} has a longitudinal part proportional to M_W^2. This causes a severe problem in the Green's function (A.11): if Π_{ZA} is not strictly proportional to q^2, the propagators pick up new nonphysical poles at $q^2 = 0$ (new long-range interactions). The longitudinal part Π_{ZA}^L corresponds to a new one-loop mass term mixing the Z and the photon, indicating that the effective "mass matrix" of the neutral current gauge bosons is *misdiagonalized.* A related problem occurs when we use (A.11) to define a running SU(2) coupling g_*^2 analogous to e_*^2 of Section 2. g_*^2 will have the form:

$$\frac{1}{g_*^2} = \frac{1}{g_0^2} - \Pi'_{3Q}(q^2) \quad , \qquad (A.12)$$

where $\Pi'_{3Q} \equiv \Pi_{3Q}/q^2$. Again, the longitudinal part means that $\Pi_{3Q}(0) \neq 0$ — the nonphysical pole reappears in a new form. Furthermore, the running of g_*^2 with q^2 is not at all what one would expect from the RNG: Π'_{3Q} does not contain the correct divergences and leading logarithms.

The root of this problem lies in another, apparently unrelated difficulty. The vector boson contributions to the Π's, unlike those of fermions and scalars, are *not* gauge-invariant alone and need to be combined with the vertex corrections to reach a correct result.[29] The vertices themselves (Figs. 8a and b) contain "extra" pieces that are not gauge-invariant and finite even when combined with the external leg self-energies. This should be contrasted with the situation in QED: there, the Ward identity guarantees that the *full* vertices (i.e., with the external leg self-energies and wavefunction renormalization) are gauge-invariant and finite. These "extra" vertex parts are directly attributable to the non–Abelian nature of the theory. Let us call them the "non–Abelian" vertex parts and call the other parts, gauge-invariant and finite, "Abelian." We will henceforth deal with the full vertices and assume that the external leg self-energies and wavefunction renormalizations are included. The non–Abelian parts appear because of the

noncommutativity of the group generators. Figure 8a is purely non–Abelian in nature. The sequence of group generators in the diagram is $T^c\, f^{abc}\, T^b$, where f^{abc} are the structure constants:

$$\begin{aligned} T^c\, f^{abc}\, T^b \;&\propto\; T^{a'}\, f^{a'bc}\, f^{abc}\;, \\ &\propto T^a\, T(V) \quad . \end{aligned} \tag{A.13}$$

$T(V)$ is the trace of the adjoint representation, the *same trace* that appears in the vector boson contribution to the Π's: $\delta^{aa'}\, T(V) = f^{abc}\, f^{a'bc}$. Figure 8b has both Abelian and non–Abelian parts. The sequence is:

$$T^b\, T^a\, T^b \;=\; \left(-\frac{1}{2}\, T(V) + C_F\right)\, T^a \quad , \tag{A.14}$$

where C_F is the fermion Casimir operator $C_F = T^b\, T^b$. The part proportional to C_F is Abelian and is clearly related to the fermion self-energies in a way exactly analogous to QED. But we are now left with the non–Abelian vertex parts proportional to $T(V)$. In a one-loop calculation (with no Dyson sum), the oblique and vertex corrections would combine in a straightforward way to eliminate this problem. Once the Dyson's sum of the oblique corrections is introduced, this connection is severed.

We can circumvent the Dyson's equation by examining the effective Lagrangian in momentum space. The appropriate parts are the bare mass terms and one-loop longitudinal self-energies of the Z and the photon. We will also need to examine the vertex functions. Starting with the SU(2) fields W_0^i, the U(1) field B_0, the fermions ψ_0 and the scalars ϕ_0:

$$\begin{aligned} \mathcal{L}_{eff} = &-\frac{1}{4}\, W^{i2}_{\mu\nu_0} - \frac{1}{4}\, B^2_{\mu\nu_0} - \sum_{\phi} |D_\mu \phi_0|^2 - \bar{\psi}_0 (\not{D} - m_0)\, \psi_0 + \frac{1}{2}\, W^i_{\mu_0}\, W^i_{\mu_0} \Pi^{ij}\, g^{ij}\;, \\ &+ i g_o \bar{\psi}_0 \left[\frac{1}{\sqrt{2}} \left(I_+ \not{W}_{-0} + I_- \not{W}_{+0}\right)\, g_0^2\, \Gamma_1 + I_3 \not{W}_3\, g_0^2 \Gamma_3\right]\, \psi_0 \;. \end{aligned} \tag{A.15}$$

D_μ is the covariant derivative; Γ_1 and Γ_3 are the fermionic charged- and neutral-current vertex corrections, explicitly shown. In fact, every vertex in the theory will pick up corrections:

$$\begin{aligned}
g_0 I_3 \not{W} &\to g_0(1+g_0^2\Gamma_3)\, I_3 \not{W}_3 \ , \\
g_0 I_\pm \not{W}_\mp &\to g_0(1+g_0^2\Gamma_1)\, I_\pm W_\mp \ , \\
g_0(\partial\phi)\phi W &\to g_0(1+g_0^2\Gamma_{W\phi\phi})\,(\partial\phi)\phi W \ , \\
g_0(\phi W)^2 &\to g_0(1+2g_0^2\Gamma_{WW\phi\phi})\,(\phi W)^2 \ , \\
g_0 WW(\partial W) &\to g_0(1+g_0^2\Gamma_{3W})\, WW(\partial W) \ , \\
g_0^2 W^4 &\to g_0^2(1+2g_0^2\Gamma_{4W})\, W^4 \ .
\end{aligned} \tag{A.16}$$

The first step to a solution is to identify the gauge-dependent part of the vertices necessary to make the self-energies gauge-invariant. Inasmuch as we are working in the R_ξ gauge, gauge dependence will manifest itself through ξ dependence. Let us divide every vertex in the theory into two parts: $\Gamma = \Gamma'(\xi) + \tilde{\Gamma}$, where the former part carries the gauge dependence and the latter does not. Each Γ will depend on its process; that is, on what type of physical, on-shell particles are coupling to the gauge bosons, be they fermions, scalars or other vector bosons. However, the part Γ' *cannot* depend on the nature of the process at the vertex because it always combines with the vector self-energies to form a gauge-invariant result. The vector boson self-energies are oblique and "do not know" about what kinds of particles are coupling at the vertices. Hence, Γ' is *universal* to all vertices. By the same token, any part of the vertex that *does* depend on the vertex process *must* be gauge-invariant, inasmuch as it has nothing else in a physical matrix element to combine with. Concisely, the gauge-dependent part $\Gamma'(\xi)$ must be universal, while the nonuniversal parts of the vertices must be gauge-invariant. Apart from any parts that are both gauge-invariant and universal (which we will deal with presently), we can write $\tilde{\Gamma} = \Gamma^{Ab} + \tilde{\Gamma}^{nAb}$ and identify the Abelian part

of the vertex completely with the process-specific, gauge-invariant part, just as in QED. The second and final step is to rediagonalize the effective mass matrix of the neutral current sector, eliminating the troublesome Π_{3Q}^{L} and also relating it to Γ'. Rewrite every vertex, then, as:

$$g_0\ \left[1+g_0^2\Gamma\right]\ \simeq\ \left[1+g_0^2\Gamma'\right]\ \left[1+g_0^2\Gamma^{Ab}+g_0^2\tilde{\Gamma}^{nAb}\right]\quad . \tag{A.17}$$

Now define a new universal coupling $\tilde{g}$:

$$\tilde{g}\ =\ g_0\left(1+g_0^2\Gamma'\right)\quad . \tag{A.18}$$

The longitudinal part of Π_{ZA} is due to the "extra" renormalization of the $\phi\phi WW$ vertex by the non–Abelian parts, where the ϕ's are interacting with the vacuum (see Fig. 9). The bare mass terms are:

$$g_0^2\left[\sum_{\phi}\left\langle\phi_0^+(\vec{I}^2-I_3^2)\,\phi_0\right\rangle_0\right]\,W_0^+W_0^-+\left[\sum_{\phi}\left\langle\phi_0^+\,I_3^2\,\phi_0\right\rangle_0\right]\,\left(g_0W_0^3-g_0'B_0\right)^2\quad , \tag{A.19}$$

where $W^{\pm}=(W^1\pm iW^2)/\sqrt{2}$. Now rediagonalize by defining a new Z and photon [see Eq. (A.1)]:

$$\begin{aligned} Z\ &=\ \left(\tilde{g}^2+g_0'^2\right)^{-1/2}\ \left(\tilde{g}W_0^3-g_0'B_0\right)\ , \\ A\ &=\ \left(\tilde{g}^2+g_0'^2\right)^{-1/2}\ \left(g_0'W_0^3+\tilde{g}B_0\right)\quad . \end{aligned} \tag{A.20}$$

The currents are now:

$$\begin{aligned} J_A\ &=\tilde{e}\,J_Q\ , \\ J_Z\ &=\frac{\tilde{e}}{\tilde{s}\tilde{c}}\ \left[J_3-\tilde{s}^2\,J_Q\right]\ , \\ J_W^{\pm}\ &=\frac{\tilde{g}}{\sqrt{2}}\,J^{\pm}\quad ; \end{aligned} \tag{A.21}$$

$$\frac{1}{\tilde{e}^2}\ =\ \frac{1}{\tilde{g}^2}+\frac{1}{g_0'^2}\ ,\qquad \tilde{e}\ =\ \tilde{g}\tilde{s}=g_o'\tilde{c}\quad . \tag{A.22}$$

The mass terms are now:

$$M_{W_0}^2 = g_0^2 \sum_{\phi} \left\langle \phi_0^+ \left(\vec{I}^2 - I_3^2 \right) \phi_0 \right\rangle_0$$
$$M_{Z_0}^2 = 2\left(\tilde{g}^2 + g_0'^2\right) \sum_{\phi} \langle \phi_0^+ I_3^2 \phi_0 \rangle_0 \quad ; \tag{A.23}$$

and the rediagonalization has induced some new self-energies in the tree-level bare Lagrangian that will be combined with the one-loop parts:

$$\Pi_{ZZ} \rightarrow \Pi_{ZZ} + 2(2\tilde{g}^2) \left(\sum_{\phi} \langle \phi_0^+ I_3^2 \phi_0 \rangle_0 \right) (g_0^2 \Gamma') ,$$
$$\Pi_{ZA} \rightarrow \Pi_{ZA} + 2(\tilde{g} g_0') \left(\sum_{\phi} \langle \phi_0^+ I_3^2 \phi_0 \rangle_0 \right) (g_0^2 \Gamma') , \tag{A.24}$$
$$\Pi_{AA} \rightarrow \Pi_{AA} ,$$
$$\Pi_{WW} \rightarrow \Pi_{WW} .$$

We fix Γ' now by forcing the new term in Π_{ZA} to cancel the already-present longitudinal part.

$$\Pi_{ZA}^L = \frac{\tilde{e}^2}{\tilde{s}\tilde{c}} \Pi_{3Q}^L , \tag{A.25}$$

since Π_{QQ} has no longitudinal part. Now

$$\Pi_{ZA}^L = \tilde{g} g_0' \Pi_{3Q}^L , \tag{A.26}$$

so that:

$$\Pi_{3Q} + 2 \left(\sum_{\phi} \langle \phi_0^+ I_3^2 \phi_0 \rangle_0 \right) g_0^2 \Gamma' \equiv \Pi_{3Q}^T = q^2 \Pi_{3Q}' ,$$
$$\sum_{\phi} \langle \phi_0^+ \ldots \phi_0 \rangle_0 = \sum \langle \ldots \rangle_0 , \tag{A.27}$$

so that the new Π_{ZA} is purely transverse. A simple check on A.27 is that Π^L_{3Q} is indeed proportional to $(2\,I_3^2)_0$, as careful consideration of Fig. 9 will show.

The Dyson's equations are now modified by a new set of rules:

1. Replace

$$g_0 \rightarrow \tilde{g}_0\,,$$

$$g_0' \rightarrow g_0'\,,$$

$$e_0 \rightarrow \tilde{e}\,,$$

$$s_0 \rightarrow \tilde{s}\,,$$

$$c_0 \rightarrow \tilde{c}\,.$$

2. Throw away Π^L_{3Q} whenever it appears in Π_{ZA}. Call the new function $\Pi^T_{3Q} = \Pi_{3Q} + \langle 2I_3^2 \rangle_0\,\Gamma'$. Remove Γ' from all vertices.

3. Insert $-2\tilde{g}^2\,\Pi^L_{3Q}$ into Π_{ZZ}.

All the problems with the Green's functions discussed above have now been solved: Π_{ZA} is purely transverse, the running SU(2) coupling g_*^2 has the correct leading logarithms (see below and Section 4), and the matrix elements are gauge-invariant. The procedure is gauge-invariant by construction. Moreover, the residual neutral current vertices $\tilde{\Gamma}_3$ have the crucial properties that they are finite and vanish at $q^2 = 0$, regardless of the Higgs vacuum structure. Γ' is of course the leftover part of the vertex that exactly cancels the longitudinal part of Π_{ZA} at $q^2 = 0$.[2,9] Hence, the electroweak neutral current vertices merge without difficulty into QED and satisfy the Abelian Ward identity requiring them to vanish at $q^2 = 0$. The full non–Abelian symmetry of SU(2) $\times$ U(1), after symmetry-breakdown, preserves the QED result that at $q^2 = 0$, the electric charge receives no renormalization (finite or infinite) other than from the oblique parts. In the counterterm approach, this symmetry would relate the

"extra" counterterm for the vertex to the counterterm necessary for Π^L_{ZA}. Normally, this counterterm is chosen to cancel $\Pi^L_{ZA}(0)$, but this is RS–dependent.[9] The superiority of the new procedure lies in fact that it is RS–independent and completely determined by the principle of gauge invariance and the requirement that the theory be expressed in terms of physical, diagonal degrees of freedom.

We can now define a set of finite, RS–invariant running couplings. Note, since Π_{QQ} and Π^T_{3Q} are purely transverse,

$$\begin{aligned} \Pi_{QQ} &= q^2\, \Pi'_{QQ} \ , \\ \Pi^T_{3Q} &= q^2\, \Pi'_{3Q} \quad . \end{aligned} \tag{A.28}$$

Then

$$\frac{1}{e_*^2} = \frac{1}{e_0^2} - \mathrm{Re}\left[\Pi'_{QQ} + 2\Gamma'\right] \quad , \tag{A.29}$$

$$s_*^2 = \mathrm{Re}\left[\frac{\frac{1}{g_0^2} - (\Pi'_{3Q} + 2\Gamma')}{\frac{1}{e_0^2} - (\Pi'_{QQ} + 2\Gamma')}\right] \quad , \tag{A.30}$$

$$\begin{aligned} \frac{1}{4\sqrt{2}\, G_{\mu_*}} = \mathrm{Re}\Bigg[& 2 \sum \langle I_3^2 \rangle_0 - \Pi_{11} + \Pi^T_{3Q} + 2\Pi^L_{3Q} \\ & + \left(\sum \langle \vec{I}^2 - 3I_3^2 \phi_0 \rangle_0\right)\left(1 + \frac{\Pi^L_{3Q}}{\sum \langle I_3^2 \rangle_0}\right)\Bigg] \quad , \end{aligned} \tag{A.31}$$

$$\frac{1}{\rho_*} = 1 - 4\sqrt{2}\, G_{\mu_*} \mathrm{Re}\left[\Pi_{33} - \Pi_{11} + \left(\sum \left\langle \vec{I}^2 - 3I_3^2 \right\rangle_0\right)\left(1 + \frac{\Pi^L_{3Q}}{\sum \langle I_3^2 \rangle_0}\right)\right] \ . \tag{A.32}$$

The "starred" functions are clearly RS–independent, being defined entirely in terms of bare quantities. We also introduce a set of RS–invariant imaginary parts:

$$\mathrm{Im}\ \Pi'^*_{AA} = e_*^2\, \mathrm{Im}\ \left(\Pi'_{QQ} + 2\Gamma'\right) \ , \tag{A.33}$$

$$\text{Im}\,\Pi'^{*}_{ZA} = \frac{e_*^2}{s_* c_*}\left[\text{Im}\left(\Pi'_{3Q} + 2\Gamma'\right) - s_*^2 \text{Im}\,\left(\Pi'_{QQ} + 2\Gamma'\right)\right] , \qquad (A.34)$$

$$\text{Im}\,\Pi^{*}_{ZZ} = \frac{e_*^2}{s_*^2 c_*^2}\,\text{Im}\,\left(\Pi_{33} - 2s_*^2\,\Pi_{3Q} + s_*^4 \Pi_{QQ} - \Pi^{L}_{3Q}\right) , \qquad (A.35)$$

$$\text{Im}\,\Pi^{*}_{WW} = \frac{e_*^2}{s_*^2}\,\text{Im}\,\left[\Pi_{11} + 2\left(q^2 + M^2_{W_0}\right)\Gamma'\right] . \qquad (A.36)$$

The imaginary parts are generally small, and we can introduce the following running SU(2) g_* and U(1) g'_* running couplings:

$$\begin{aligned} \frac{1}{g_*^2} &= \frac{1}{g_0^2} - \text{Re}\left(\Pi'_{3Q} + 2\Gamma'\right) , \\ \frac{1}{g'^2_*} &= \frac{1}{g'^2_0} - \text{Re}\left(\Pi'_{QQ} - \Pi'_{3Q}\right) , \end{aligned} \qquad (A.37)$$

which have the usual asymptotic RNG behavior. (Note, however, the g' differs from the g_1 used in GUTs by a Clebsch–Gordon coefficient.) The neutral- and charged-current matrix elements now appear in especially simple form when written in terms of these functions. Apart from box and residual ($\tilde{\Gamma}$) vertex loops:

$$\begin{aligned} \mathcal{M}_{NC} &= \frac{e_*^2 Q Q'}{q^2\left[1 - i\text{Im}\,\Pi'^{*}_{AA}\right]} + \left(\frac{e_*^2}{s_*^2 c_*^2}\right) \\ &\times \frac{\left[I_3 - \left(s_*^2 - i s_* c_*\,\text{Im}\,\Pi'^{*}_{ZA}\right) Q\right]\left[I'_3 - \left(s_*^2 - i s_* c_*\,\text{Im}\,\Pi'^{*}_{ZA}\right) Q'\right]}{q^2\left[1 + i\left(\text{Im}\,\Pi'^{*}_{AA}\right)^2\right]\left[1 + \frac{\lambda}{s_*^2 c_*^2}\right] + \frac{e_*^2}{4\sqrt{2}\, s_*^2 c_*^2 G_{\mu_*}\rho_*} - i\sqrt{s}\,\Gamma_{Z_*}} ; \end{aligned} \qquad (A.38)$$

$$\mathcal{M}_{CC} = \frac{e_*^2}{s_*^2}\,\frac{\langle I_+ I_- \rangle}{q^2\left[1 - \frac{c_*}{s_*}\left(\text{Im}\,\Pi'^{*}_{AA}\right)\left(\text{Im}\,\Pi'^{*}_{ZA}\right)\right] + \frac{e_*^2}{4\sqrt{2}\, s_*^2 G_{\mu_*}} - i\sqrt{s}\,\Gamma_{W_*}} . \qquad (A.39)$$

We have introduced some auxiliary functions:

$$\begin{aligned}
\lambda &= \frac{(e_*^2 \,\mathrm{Im}\, \Pi'_{3Q})^2 - (e_*^2 \,\mathrm{Im}\, \Pi'_{3Q})\,(\mathrm{Im}\, \Pi'^*_{AA})}{1 + (\mathrm{Im}\, \Pi'^*_{AA})^2} \,, \\
\sqrt{s}\,\Gamma_{Z*} &= \mathrm{Im}\, \Pi^*_{ZZ} + q^2 (\mathrm{Im}\, \Pi'^*_{AA})(\mathrm{Im}\, \Pi'^*_{ZA}) \,, \\
\sqrt{s}\,\Gamma_{W*} &= \mathrm{Im}\, \Pi^*_{WW} \quad ;
\end{aligned} \tag{A.40}$$

$s = -q^2$ for timelike q^2, $c_*^2 = 1 - s_*^2$.

We now complete the calculation by choosing inputs at given values of q^2 to fix the starred functions. This choice is the analogue of a RS. The definitions A.29–A.32 can then be used to run the functions from that q^2 to any other. In this paper we choose the scheme introduced in Ref. 2 with the free parameters: α, G_μ, M_Z, ρ. G_μ is the usual muon decay constant, α is the long-range ($q^2 = 0$) electromagnetic coupling, M_Z is the Z^0 mass and ρ is the $q^2 = 0$ ρ–parameter measured, for example, in νN scattering. Once fixed by experiment, these parameters can then be put into the starred functions. Clearly:

$$\begin{aligned}
e_*^2(0) &= 4\pi\alpha \,, \\
G_{\mu *}(0) &= G_\mu \,, \\
\rho_*(0) &= \rho \quad .
\end{aligned} \tag{A.41}$$

The Z mass can be used to fix the value of s_*^2 at the Z pole:

$$s_*^2 c_*^2 \big|_Z = \left. \frac{e_*^2}{4\sqrt{2}\, M_Z^2\, G_{\mu *}\, \rho_*} \right|_Z \left. \frac{1}{1 + (\mathrm{Im}\Pi'^*_{AA})^2} \right|_Z - \lambda|_Z \,. \tag{A.42}$$

(The definitions A.41 are not quite complete: there are still small vertex and box corrections that need to be included in them; see below.) Using these inputs, and defining:

$$\Delta_Q(q^2) = \mathrm{Re}\left[\Pi'_{QQ}(q^2) + 2\Gamma'(q^2)\right] - \mathrm{Re}\left[\Pi'_{QQ}(0) + 2\Gamma'(0)\right] , \qquad (A.43)$$

$$\Delta_3(q^2) = \mathrm{Re}\left\{\Pi_{33}(q^2) - \Pi^T_{3Q}(q^2) - \Pi_{33}(0) - 2\left[\Pi^L_{3Q}(q^2) - \Pi^L_{3Q}(0)\right]\right\} , \qquad (A.44)$$

$$\Delta_1(q^2) = \mathrm{Re}\left\{\Pi_{11}(q^2) - \Pi^T_{3Q}(q^2) - \Pi_{11}(0) + 2M^2_{W_0}\left[\Gamma'(q^2) - \Gamma'(0)\right]\right\} , \qquad (A.45)$$

$$\Delta_\rho(q^2) = \Delta_3 - \rho^{-1}\,\Delta_1 ; \qquad (A.46)$$

we have:

$$e^2_*(q^2) = \frac{e^2}{1 - e^2\Delta_Q(q^2)} , \qquad (A.47)$$

$$G_{\mu *}(q^2) = \frac{G_\mu}{1 - 4\sqrt{2}\,G_\mu\,\Delta_1(q^2)} , \qquad (A.48)$$

$$\rho_*(q^2) = \frac{\rho}{1 - 4\sqrt{2}\,\rho G_{\mu *}\,\Delta_\rho(q^2)} . \qquad (A.49)$$

s^2_* is controlled by the evolution equation:

$$\begin{aligned}\left[1 + (\mathrm{Im}\,\Pi'^*_{AA})^2\right]\,\left.\frac{s^2_*}{e^2_*}\right|_q - \left[1 + (\mathrm{Im}\,\Pi'^*_{AA})^2\right]\,\left.\frac{s^2_*}{e^2_*}\right|_Z = \\ \mathrm{Re}\left[\Pi'_{3Q}(q^2) + 2\Gamma'(q^2) - \Pi'_{3Q}(Z) - 2\Gamma'(Z)\right] \qquad (A.50) \\ + \,(\mathrm{Im}\,\Pi'^*_{AA})\left[\mathrm{Im}\,\left(\Pi'_{3Q} + 2\Gamma'\right)\right]\Big|_q - \,(\mathrm{Im}\,\Pi'^*_{AA})\left[\mathrm{Im}\,\left(\Pi'_{3Q} + 2\Gamma'\right)\right]\Big|_Z .\end{aligned}$$

The contributions from the imaginary parts are small. The bare masses appearing in the one-loop corrections can be replaced by their physical values, inasmuch as the differences are of higher order in the irreducible loop expansion. Then the starred functions and the matrix elements are not only RS–independent but finite as well. Furthermore, it is easy to show that to one loop, the Γ' cancels from the denominators of M_{NC} and M_{CC} at the respective poles, as required by the LSZ formula.

In the standard model, with one Higgs doublet, $\rho_0 = 1$, and we have

$$\Pi^L_{3Q} + M^2_{W_0}\Gamma' \;=\; 0 \quad , \tag{A.51}$$

so:

$$\begin{aligned}
\Delta_1(q^2) \;&=\; \mathrm{Re}\left\{\Pi_{11}(q^2) - \Pi^T_{3Q}(q^2) - \Pi_{11}(0) - 2\left[\Pi^L_{3Q}(q^2) - \Pi^L_{3Q}(0)\right]\right\} \;, \\
\Delta_\rho(q^2) \;&=\; \mathrm{Re}\left[\Pi_{33}(q^2) - \Pi_{11}(q^2)\right] \quad ,
\end{aligned} \tag{A.52}$$

and

$$\rho_*(q^2) \;=\; \frac{1}{1 - 4\sqrt{2}\, G_{\mu *}\, \Delta_\rho(q^2)} \quad . \tag{A.53}$$

The definitions A.47, A.48 and A.50 are unchanged. Note that $\rho_*(0)$ is no longer a free parameter, but computable, corresponding to the fact that $\rho_0 = 1$. The standard model requires only three parameters to define the gauge sector: α, G_μ and M_Z.

In the computations presented in the text of this paper, we have consistently used for M_W in the one-loop corrections the true value:

$$M^2_W \;=\; \left.\frac{e^2_*}{4\sqrt{2}\; s^2_*\, G_{\mu *}}\right|_{q^2 = -M^2_W} \quad . \tag{A.54}$$

This computation of M_W (the charged current pole) is performed iteratively, beginning with a RS:

$$\begin{aligned}
\alpha \;&=\; (137.03602)^{-1} \;, \\
G_\mu \;&=\; 1.16637 \times 10^{-5}\ \mathrm{GeV}^{-2} \quad ,
\end{aligned} \tag{A.55}$$

and some value of M_Z. (We assume $\rho_0 = 1$.) A "tree-level" s_θ, c_θ and M_W are defined:

$$
\begin{aligned}
s_\theta^2 &= \frac{1}{2}\left[1-\sqrt{1-\frac{4\pi\alpha}{\sqrt{2}\,G_\mu M_Z^2}}\;\right], \\
c_\theta^2 &= 1-s_\theta^2\,, \\
M_W &= c_\theta M_Z \quad ,
\end{aligned}
\tag{A.56}
$$

and are used as seeds to begin the calculation. At every step, we redefine:

$$
c_\theta^2 = \frac{M_W}{M_Z}\,, \qquad M_W \text{ used in loops } = \text{ last computed value.} \tag{A.57}
$$

M_W is computed to some specified accuracy (1 MeV in this paper) and is then used (along with the new c_θ, s_θ) for all subsequent calculations. In this way, the masses appearing in the radiative correction loops are the physical RS–invariant masses. A computer program, SSTAR, has been developed by one of us (DCK) at SLAC to compute the starred functions using this procedure.

The fermion masses are:

$$
\begin{array}{llll}
m_u = 4.5 \text{ MeV} & m_c = 1.35 \text{ GeV} & & \\
m_d = 7.9 \text{ MeV} & m_s = 155 \text{ MeV} & m_b = 5.3 \text{ GeV} & \\
m_{\nu_e} = 0 & m_{\nu_\mu} = 0 & m_{\nu_\tau} = 0 & \\
m_e = 0.511 \text{ MeV} & m_\mu = 105.6 \text{ MeV} & m_\tau = 1.784 \text{ GeV}\,. &
\end{array}
\tag{A.58}
$$

The quark masses are current masses.[30] The top and Higgs masses are free parameters. For the hadronic contribution to Π'_{QQ} and Π'_{3Q}, we use dispersion relations.[14,31] The fermion wavefunctions are bare, while the incoming and outgoing particles are physical and on-shell, or "dressed." The two must be related in the matrix element by the external field, or wavefunction, renormalizations: $\psi_0 = Z_F^{1/2}\psi$, where ψ_0 is the bare and ψ the physical fermion. Z_F is the rescaling obtained from on-shell renormalization. It should be stressed, however, that this relationship is *not* a RS, but a statement connecting bare and physical particles.

The same reasoning applies if we use other particles, such as vector bosons.[27] In our treatment, we omit the photonic contribution because of the infrared divergence; it must be handled separately by the usual QED techniques. In the standard model:

$$Z_L = 1 - \frac{g_0^2}{16\pi^2}\left\{\frac{1}{2}\left[(\Delta - \ell n\, M_W^2) - \frac{1}{2}\right] + \left(\frac{I_3 - s_0^2 Q}{c_0}\right)^2\left[(\Delta - \ell n\, M_Z^2) - \frac{1}{2}\right]\right\} ,$$

$$Z_R = 1 - \frac{g_0^2}{16\pi^2}\left\{\left(-\frac{s_0^2 Q}{c_0}\right)^2\left[(\Delta - \ell n\, M_Z^2) - \frac{1}{2}\right]\right\} \quad . \tag{A.59}$$

To specify the RS more carefully, we note that there are residual vertex and box corrections to the input parameters. The box correction to α is taken into account in its experimental definition. The fermion vertices are given in Appendix B, with the photonic parts deleted. The Abelian vertex is combined in the usual way with external self-energies and wavefunction renormalization (A.58) to give a finite result. Recall also that $\tilde{\Gamma}_3$ is finite and zero at $q^2 = 0$, as discussed above. G_μ, on the other hand, does have residual corrections not included in its definition. The traditional photonic corrections to the muon lifetime give:

$$\tau_\mu^{-1} = \frac{G_\mu^2 m_\mu^5}{192\pi^3}\left(1 - \frac{8m_e^2}{m_\mu^2}\right)\left[1 + \frac{3}{5}\frac{m_\mu^2}{M_W^2} + \frac{\alpha}{2\pi}\left(\frac{25}{4} - \pi^2\right)\right] \quad . \tag{A.60}$$

These corrections include the W–photon boxes and the infrared parts of the photonic vertex corrections, with the infrared divergence separated as follows. The photon propagator is rewritten:

$$\frac{1}{k^2} = \frac{1}{k^2}\frac{M_W^2}{k^2 + M_W^2} + \frac{1}{k^2 + M_W^2} \quad , \tag{A.61}$$

$$\gamma = \qquad \gamma_< + \qquad \gamma_> \quad .$$

Only the part $\gamma_<$ is included in the vertices.[82] Left out are the Z–W boxes and all the other vertex corrections: $\gamma_>$ and Z. This means that G_μ and $G_{\mu*}(0)$ are not precisely the same:

$$
\begin{aligned}
G_{\mu*}(0) &= G_\mu \left[1 + \delta_{\rm ver} + \delta_{\rm box}\right]^{-1} , \\
\delta_{\rm ver} &= \Gamma_1^{\rm full} - (\gamma_< \text{ contribution}) - \Gamma' \Big|_{q^2=0} , \\
&= \frac{\alpha}{2\pi s_\theta^2} \left[3 - \left(c_\theta^2 - 3\frac{c_\theta^2}{s_\theta^2}\right) \ell n\, c_\theta^2\right] , \\
\delta_{\rm box} &= -\frac{\alpha}{8\pi} \left(5\frac{c_\theta^4}{s_\theta^4} - 3\right) \ell n\, c_\theta^2 \quad .
\end{aligned}
\tag{A.62}
$$

Appendix B. Proper Self–Energies and Non–Abelian Vertices

In this appendix we present the proper self-energies Π and non–Abelian vertices Γ to one loop for the standard model, with $\xi = 1$ in the R_ξ gauge, with one Higgs doublet and $\rho_0 = 1$.[2,9,33] Define with Passarino and Veltman[8] the following form factors with dimensional regularization:

$$A(m^2) = \int \frac{d^4k}{i\pi^2} \frac{1}{k^2 + m^2 - i\epsilon} \quad ,$$

$$\{B_0,\ B_\mu,\ B_{\mu\nu}\}\ (q^2;\ m_1^2\ m_2^2) = \int \frac{d^4k}{i\pi^2} \frac{\{1,\ k_\mu,\ k_\mu\ k_\nu\}}{[k^2 + m_1^2 - i\epsilon][(k+q)^2 + m_2^2 - i\epsilon]}$$

$$B_\mu = q_\mu\ B_1 \qquad (B.1)$$

$$B_{\mu\nu} = q_\mu\ q_\nu\ B_{21} + \delta_{\mu\nu}\ B_{22},\ B_3 = B_{21} + B_1 \quad .$$

The factors B_0, B_1, B_{21} are logarithmically divergent, A and B_{22} quadratically divergent. A and B_{22} must eventually cancel from any Π or Γ, leaving only logarithmic divergences. The Feynman parametrization of the functions B_0, B_1, B_{22} are:

$$B_0 = \Delta - \int_0^1 dx \ell n\ [m_1^2 + (q^2 + m_2^2 - m_1^2)x - x^2\ q^2 - i\epsilon]$$

$$B_1 = -\frac{1}{2}\Delta + \int_0^1 dx\ x\ \ell n\ [m_1^2 + (q^2 + m_2^2 - m_1^2)x - x^2\ q^2 - i\epsilon] \qquad (B.2)$$

$$B_{21} = \frac{1}{3}\Delta - \int_0^1 dx\ x^2\ \ell n\ [m_1^2 + (q^2 + m_2^2 - m_1^2)x - x^2\ q^2 - i\epsilon] \quad ,$$

where

$$\Delta = \frac{2}{4-n} - \gamma - \ell n\pi \quad , \qquad (B.3)$$

and γ is the Euler–Mascheroni constant. The dimension n approaches 4. The B's can be expressed in closed form for numerical evaluation.[9]

Equations B.4–B.7 give the gauge boson/scalar contributions, equations B.8–B.11 the fermion contributions. In the following "f" means all fermions and "D" means all doublets of fermions. Fermion sums contain a factor of three for quarks implicitly.

Gauge Bosons/Scalars[9]

$$\begin{aligned}16\pi^2\ \Pi_{33}(q^2) = q^2 &\left[-9B_3(W,W) + \frac{7}{4}\ B_0(W,W) + \frac{2}{3}\right] - 2M_W^2\ B_0(W,W) \\ &+ \frac{1}{4}(M_Z^2 - M_H^2)\ [2B_1(Z,H) + B_0(Z,H)] \\ &- \frac{1}{4}\ q^2[4B_3(Z,H) + B_0(Z,H)] + M_Z^2\ B_0(Z,H)\end{aligned} \tag{B.4}$$

$$\begin{aligned}16\pi^2\ \Pi_{11}(q^2) = &\frac{2}{3}q^2 + s_\theta^2\left\{q^2[-8B_3 + 2B_0] + 2M_W^2[2B_1 + B_0]\right\}\ (W,0) \\ &+ c_\theta^2\left\{q^2[-8B_3 + 2B_0] + 2(M_W^2 - M_Z^2)[2B_1 + B_0\right\}\ (W,Z) \\ &+ \left\{q^2[-B_3 - (1/4)B_0] + (1/4)(M_W^2 - M_Z^2)\ [2B_1 + B_0]\right\}\ (W,Z) \\ &+ (M_Z^2 - 3M_W^2)\ B_0\ (W,Z) \\ &+ \frac{1}{4}(M_W^2 - M_H^2)\ [2B_1(W,H) + B_0(W,H)] \\ &- \frac{1}{4}q^2[4B_3(W,H) + B_0(W,H)] + M_W^2 B_0(W,H)\end{aligned} \tag{B.5}$$

$$\begin{aligned}16\pi^2\ \Pi_{3Q}^T(q^2)&\left[-10\ B_3(W,W) + \frac{3}{2}\ B_0(W,W) + \frac{2}{3}\right]\ , \\ 16\pi^2\ \Pi_{3Q}^L(q^2) &= -2M_W^2\ B_0(W,W)\end{aligned} \tag{B.6}$$

$$16\pi^2\ \Pi_{QQ}(q^2) = q^2\left[-12\ B_3(W,W) + B_0(W,W) + \frac{2}{3}\right] \tag{B.7}$$

$$W = M_W,\ Z = M_Z,\ H = M_H\ .$$

Fermions[9]

$$16\pi^2\ \Pi_{33}(q^2) = 2\ \Sigma_f\ I_{3_f}^2\ [2q^2\ B_3(f,f) - m_f^2 B_0(f,f)] \qquad (B.8)$$

$$16\pi^2\ \Pi_{11}(q^2) = \Sigma_D\ 2q^2\ B_3(1,2) + m_1^2\ B_1(2,1) + m_2^2\ B_1(1,2) \qquad (B.9)$$

$$16\pi^2\ \Pi_{3Q}(q^2) = 4q^2\ \Sigma_f\ Q_f\ I_{3_f}\ B_3(f,f) \qquad (B.10)$$

$$16\pi^2\ \Pi_{QQ}(q^2) = 8q^2\ \Sigma_f\ Q_f^2\ B_3(f,f) \qquad (B.11)$$

$$f = m_f,\ 1,2 = m_{1,2}$$

$$I_{3_f},\ Q_f = \text{isospin, charge} \quad .$$

Vertex Parts[9,33]

$$\begin{aligned} 16\pi^2\ \Gamma_3^{Ab}(q^2) = \gamma_+ &\left(\frac{I_3 - s_\theta^2 Q}{c_\theta}\right)^2\ \Phi\ (Z) \\ &+ \gamma_- \left(\frac{-s_\theta^2 Q}{c_\theta}\right)^2\ \Phi\ (Z) + \frac{1}{2}\ \gamma_+ \Phi(W) \quad , \end{aligned} \qquad (B.12)$$

$$16\pi^2\ \Gamma_3^{nAb}(q^2) = -\gamma_+[\Phi(W) + \Lambda(W) - 16\pi^2\ \Gamma'(q^2=0)] \quad , \qquad (B.13)$$

where γ_+ = left-handed Dirac projector and γ_- = right-handed Dirac projector. $I_3,\ Q$ = external isospin, charge.

$$\begin{aligned} \Phi(M) = \frac{1}{2} &- ln(-u - i\epsilon) + 4\left[1 + \frac{1}{2u}\right][ln(-u - i\epsilon) - 1] \\ &- 2\left(1 + \frac{1}{u}\right)^2 \left[\frac{1}{6}\pi^2 - Sp(1 + u + i\epsilon)\right] \quad , \end{aligned} \qquad (B.14)$$

$$\Lambda(M) = -\frac{5}{2} + \frac{2}{u} + \left(1 + \frac{2}{u}\right)\ l\ \sqrt{1 - \frac{4}{u}} + \left(1 + \frac{1}{2u}\right)\frac{4}{u}\ l^2 \quad ;$$

$$u = -\,q^2/M^2$$
$$l = ln\left[\sqrt{1-\frac{4}{u}}-1+i\epsilon/\sqrt{1-\frac{4}{u}}+1+i\epsilon\right] \quad , \tag{B.15}$$

where Sp = Spence function.

$$\Gamma_3^{nAb}(q^2) = \Gamma'(q^2) + \tilde{\Gamma}^{nAb}(q^2) \quad ,$$
$$16\pi^2\ \Gamma'(q^2) = 2B_0(W,W) \quad , \tag{B.16}$$
$$\Pi_{3Q}^{L} + M_W^2\ \Gamma' = 0 \quad .$$

It is useful to know something about the general behavior of the form factors. If $|q^2|,\ |m_1^2 - m_1^2| \ll m_1^2,\ m_2^2$, then:

$$B_0 = \Delta - \ell n\ m_1^2 - \frac{1}{2}\ \frac{q^2}{m_1^2}\ \left[\frac{1}{3}+\frac{m_2^2-m_1^2}{m_1^2}\right] \quad ,$$
$$B_1 = -\frac{1}{2}\ [\Delta - \ell n\ m_1^2] + \frac{1}{3}\ \frac{q^2}{m_1^2}\ \left[\frac{1}{4}+\frac{m_2^2-m_1^2}{m_1^2}\right] \quad , \tag{B.17}$$
$$B_{21} = \frac{1}{3}\ [\Delta - \ell n\ m_1^2] - \frac{1}{4}\ \frac{q^2}{m_1^2}\ \left[\frac{1}{5}+\frac{m_2^2-m_1^2}{m_1^2}\right] \quad .$$

If $|q^2| \gg m_1^2,\ m_2^2$, then:

$$B_0 = \Delta - \ell n\ (-q^2) + \left[\frac{m_1^2}{q^2}\right]\ \ell n\ \left[-\frac{m_1^2}{q^2}\right] - \frac{m_1^2}{q^2} + \left[\frac{m_2^2}{q^2}\right]\ ln\ \left[\frac{m_2^2}{q^2}\right] - \frac{m_2^2}{q^2} + 2 \quad ,$$
$$B_1 = -\ \frac{1}{2}\ [\Delta - \ell n(-q^2)] + \frac{m_1^2}{q^2} - \left[\frac{m_2^2}{q^2}\right]\ \ell n\ \left[-\frac{m_2^2}{q^2}\right] - 1 \quad , \tag{B.18}$$
$$B_{21} = \frac{1}{3}\ [\Delta - \ell n(-q^2)] + \frac{1}{2}\ \left[\frac{m_2^2}{q^2} - \frac{m_1^2}{q^2}\right] + \left[\frac{m_2^2}{q^2}\right]\ \ell n\ \left[-\frac{m_2^2}{q^2}\right] + \frac{13}{18} \quad ,$$

for q^2 timelike. If $|q^2| \ll M^2$,

$$\Phi(M) = -3q^2/M^2 \quad , \tag{B.19}$$
$$\Lambda(M) = -q^2/2M^2 \quad .$$

If $|q^2| \gg M^2$,

$$\begin{aligned} \Phi(M) &= 3ln\ (-q^2/M^2) + 2ln^2(-q^2/M^2) \\ \Lambda(M) &= -ln(-q^2/M^2) \quad , \end{aligned} \tag{B.20}$$

for q^2 timelike.

Appendix C. Gauge Boson Widths in Breit–Wigner Form

Schematically, the gauge boson propagators look like:

$$\frac{1}{q^2[1+\omega_*(q^2)]+f_*(q^2)-i\sqrt{s}\,\Gamma_*(q^2)} \quad , \quad s=-q^2 \quad ; \qquad (C.1)$$

Γ_* is defined in A.40. Numerically, ω_* is very small, $\sim 10^{-4}-10^{-3}$. Hence, we can put the resonance in the form:

$$\frac{1}{(q^2+M^2)[1+\kappa_*]-i\sqrt{s}\,\Gamma_*(q^2)} \quad , \qquad (C.2)$$

$$\kappa_* = \frac{f_*(q^2)-M^2}{q^2+M^2} \quad , \qquad (C.3)$$

and M is the physical mass:

$$M^2 = f_*(q^2)\Big|_{q^2=-M^2} \quad . \qquad (C.4)$$

Near the resonance pole, we can approximate to good accuracy:

$$\kappa_*(q^2) \to \kappa_*(-M^2) = \frac{\partial f_*}{\partial q^2}\Big|_{q^2=-M^2} \quad , \qquad (C.5)$$

and rewrite the resonance as:

$$\frac{1}{(q^2+M^2)[1+\kappa_*(-M^2)]-is\left[\frac{\Gamma_*(-M^2)}{\sqrt{s}}\right]} \quad , \qquad (C.6)$$

which can be conveniently fit to experimental data with three free parameters: M^2, $\kappa_*(-M^2)$ and $\Gamma_*/\sqrt{s}$.

The resonance form C.6 contains three important radiative effects. The *first* is the overall phase space factor of s in the width, often ignored in definitions of the Breit–Wigner shape. Note that Γ_* has also the typical fermionic phase space factors such as $1-4m^2/s$ and $1+2m^2/s$; for all but the top quark, these terms are unity. The *second* effect is due to what should be called true quantum corrections to the width; that is, renormalizations of the couplings e_*^2, s_*^2 and c_*^2. In particular, Γ_{Z_*} has an overall factor of $e_*^2/s_*^2c_*^2$, and the leading logarithms of vacuum polarization in this factor increase it by about 7% over the "tree-level" value $4\pi\alpha/s_\theta^2c_\theta^2$, if the Sirlin–Marciano s_θ^2 is used.[34] A heavy top, of course, decreases $s_*^2(Z)$, increasing the width. (Similar effects occur in the W width, proportional to e_*^2/s_*^2.) In Fig. 27 we show $\Gamma_{Z_*}(Z)$ as a function of m_t to illustrate the top's indirect effect on the width even when the Z is below the toponium threshold. (Recall, however, that the $e_*^2/s_*^2c_*^2$ cancels in the full amplitude at the Z pole.) The *third* radiative effect is the factor $1+\kappa_*$. If we are concerned with the shape of the resonance and not its overall normalization, $1+\kappa_*$ can be factored from the denominator; then the resonance contains a modified width:

$$\frac{(1+\kappa_*)^{-1}}{q^2+M^2-is\left(\frac{\widetilde{\Gamma}_*}{\sqrt{s}}\right)} \quad , \quad \widetilde{\Gamma}_* = \Gamma_*/(1+\kappa_*) \quad , \tag{C.7}$$

and the width as defined experimentally from a line shape would be increased further. (κ_* is negative in general.) In the standard model, κ_* lies between 1% and 2% for both the W and the Z. Note:

$$\begin{aligned} \kappa_{Z_*}(Z) &= \frac{\partial}{\partial q^2}\,\frac{e_*^2}{s_*^2c_*^2}\frac{1}{4\sqrt{2}G_{\mu *}\rho_*}\Big|_Z \quad , \\ \kappa_{W_*}(W) &= \frac{\partial}{\partial q^2}\,\frac{e_*^2}{s_*^2}\,\frac{1}{4\sqrt{2}G_{\mu *}}\Big|_W \quad . \end{aligned} \tag{C.8}$$

The bulk of both κ's is due to the running of the couplings e_*^2, s_*^2 and c_*^2, and this fact can be used to estimate them. At the Z and W poles, the vector boson contributions have not kicked in yet to the running, so we simply assume

N_g generations of fermions in the logarithmic regime. (We assume a light top quark.) Then:

$$\kappa_{Z*}(Z) \simeq -\frac{e_*^2}{s_*^2 c_*^2}\left[\beta C_*^4 + \beta' S_*^4\right]\Big|_Z \quad ,$$
$$\kappa_{W*}(W) \simeq -\frac{e_*^2}{s_*^2}\,\beta\Big|_W \quad ; \qquad (C.9)$$
$$\beta = 4N_g/48\pi^2 \quad , \quad \beta' = (20N_g/3)/48\pi^2 \quad .$$

The κ's are sensitive to the presence of heavy physics. In Fig. 28 we show $\kappa_{Z_*}(Z)$ as a function of m_t. The rapid decrease of κ_{Z*} is caused by the decoupling of the heavier top from the running of the couplings. The heavy top also affects the overall normalization of κ_{Z_*}, however, through $s_*^2(Z)$, and this pushes $\kappa_{Z_*}(Z)$ slowly back up for a very large top mass.

Below the $2W$ threshold, the Z width has the following form:[2]

$$\frac{\Gamma_{Z*}}{\sqrt{s}} = \frac{e_*^2}{12\pi s_*^2 c_*^2}\sum_f \left[\left(\frac{I_{3f}}{2} - Q_f s_*^2\right)^2\left(1 - \frac{2m_f^2}{q^2}\right)\right.$$
$$\left. + \left(\frac{I_{3f}}{2}\right)^2\left(1 + \frac{4m_f^2}{q^2}\right)\right]\cdot\sqrt{1+\frac{4m_f^2}{q^2}}\cdot C_{QCD} \quad , \qquad (C.10)$$
$$C_{QCD} = 1 \text{ for leptons} \quad ,$$
$$= 3\cdot\left(1 + \frac{\alpha_s(q^2)}{\pi}\right) \text{ for quarks} \quad ; \quad s = -q^2 \quad ;$$

"f" stands for sum over all accessible fermions. The W width due to fermion pairs (f, f') is:[2]

$$\frac{\Gamma_{W*}}{\sqrt{s}} = \frac{e_*^2}{48\pi s_*^2}\sum_{f,f'}\left[1 - \frac{1}{2}(\delta_f + \delta_f) + \frac{1}{2}(\delta_f - \delta_{f'})^2\right]$$
$$\left[1 - 2(\delta_f + \delta_{f'}) + (\delta_f - \delta_{f'})^2\right]^{1/2}\cdot C_{QCD} \quad , \quad \delta_f = -m_f^2/q^2 \quad ; \qquad (C.11)$$

Kobayashi–Maskawa mixing has been ignored.

The form C.6 can be used in fitting, for example, the Z line shape to determine the Z width and mass. However, in an actual experiment, the Z channel interferes with the ever-present photon channel. In principle, then, one needs to know the relative normalization [i.e., $s_*^2(Z)$] of the Z to the photon matrix element *before* one can determine the Z mass and width. (This problem becomes more subtle and complicated with bremsstrahlung.) As the Z peak is many times higher than the photon term in the neutral current, this effect is probably not large; however, it will be explored numerically in a subsequent paper.[13] Note that this difficulty does not occur with the W line shape.

REFERENCES

1. W. Hollik and H. Timme, Z. fur Physik **C33**, 125 (1986).
2. B. W. Lynn, M. E. Peskin and R. G. Stuart, SLAC–PUB–3725 (1985); LEP *Yellow Book,* CERN 86–02 (1986), Vol. I, p. 90; B. W. Lynn and R. G. Stuart, Nucl. Phys. **B253**, 216 (1985).
3. T. P. Cheng and L. F. Li, *Gauge Theory of Elementary Particle Physics* (Oxford University Press, New York, 1984), Chapters 2 and 3.
4. E. C. G. Stueckelberg and A. Petermann, Helv. Phys. Acta **26**, 499 (1953); M. Gell–Mann and F. E. Low, Phys. Rev. **95**, 1300 (1954); C. G. Callan Jr., Phys. Rev. **D2**, 1541 (1970); K. Symanzik, Comm. Math. Phys. **18**, 227 (1970).
5. F. J. Dyson, Phys. Rev. **75**, 1736 (1949).
6. S. Coleman and E. Weinberg, Phys. Rev. **D7**, 1888 (1973).
7. H. Georgi, *Weak Interactions and Modern Particle Theory* (Benjamin/ Cummings, Inc., Menlo Park, California, 1984).
8. G. Passarino and M. Veltman, Nucl. Phys. **B160**, 151 (1979).
9. R. G. Stuart, D. Phil. Thesis, Oxford University (1985).
10. S. Weinberg, Phys. Rev. **118**, 838 (1960).
11. S. Glashow, Nucl. Phys. **22**, 579 (1961); S. Weinberg, Phys. Rev. Lett. **19**, 1264 (1967); A. Salam, in *Elementary Particle Physics,* ed. N. Svartholm; Almqvist and Wiksell, Stockholm, Sweden (1968) p. 367.
12. W. Marciano and A. Sirlin, Nucl. Phys. **B189**, 442 (1981); Phys. Rev. **D22**, 2695 (1980).
13. D. C. Kennedy, R. H. Kleiss, B. W. Lynn, R. G. Stuart and J. C. Im, SLAC–PUB–4128 (1988), in preparation.
14. B. W. Lynn, G. Penso and C. Verzegnassi, Phys. Rev. **D35**, 42 (1987).

15. D. C. Kennedy and B. W. Lynn, in preparation.

16. H. Georgi, H. R. Quinn and S. Weinberg, Phys. Rev. Lett. **33,** 451 (1974).

17. J. Appelquist and J. Carazzone, Phys. Rev. **D11,** 2856 (1975).

18. J. Collins, *Renormalization* (Cambridge University Press, Cambridge, England, 1984), Chapter 8.

19. M. Veltman, Nucl. Phys. **B123,** 89 (1977).

20. W. Marciano, Nucl. Phys. **B84,** 132 (1975).

21. J. C. Collins, F. Wilczek and A. Zee, Phys. Rev. **D11,** 242 (1978).

22. M. Einhorn, D. Jones and M. Veltman, Nucl. Phys. **B191,** 146 (1981).

23. U. Amaldi, A. Bohm et al., U. of Pennsylvania UPR–0331T (1987).

24. M. K. Gaillard, in *Proc. Electroweak Symmetry Breaking Workshop,* Berkeley, California, 1984, p. 18; in *Proc. on the Physics of the Superconducting Super Collider,* Snowmass, Colorado, 1986, pp. 757–846.

25. M. Cvetic and B. W. Lynn, Phys. Rev. **D35,** 51 (1987).

26. B. W. Lynn and C. Verzegnassi, SLAC–PUB–3967 (1986).

27. C. Ahn, B. W. Lynn, M. E. Peskin and S. Selipsky, in preparation.

28. L. Baulieu and R. Coquereaux, Ann. Phys. **140,** 163 (1982).

29. C. Itzykson and J.–B. Zuber, *Quantum Field Theory* (McGraw–Hill, New York, New York, 1980), Chapter 12.

30. H. Leutwyler and J. Glasser, Phys. Rep. **87,** 77 (1982).

31. H. Burkhardht, TASSO Note #192 (1981).

32. A. Sirlin, Phys. Rev. **D22,** 971 (1980).

33. B. Grzadkowski et al., Nucl. Phys. **B281,** 18 (1987).

34. W. Wetzel, LEP *Yellow Book,* CERN 86–02 (1986), Vol. I, p. 40.

TABLE CAPTIONS

I. $\rho_*(0)$ as a function of the top (m_t) and Higgs (m_H) masses. All masses in GeV.

II. $\rho_*(q^2)$ from 1 MeV to 1 TeV in timelike energy, evaluated for different values of the top mass m_t. All masses and energies in GeV.

III. $G_{\mu_*}(Z)$ as a function of the top (m_t) and Higgs (m_H) masses. G_{μ_*} in units of 10^{-5} GeV^{-2}. All masses in GeV.

IV. ${s_*}^2(Z)$ as a function of the Z vector boson (M_Z) and top (m_t) masses. All masses in GeV.

V. ${s_*}^2(q^2)$ from 1 MeV to 1 TeV in timelike energy, evaluated for different values of the top mass m_t. All masses and energies in GeV.

VI. The W vector boson mass as a function of the Z vector boson (M_Z) and top (m_t) masses. All masses in GeV.

VII. The W vector boson mass as a function of the Z vector boson (M_Z) and Higgs (m_H) masses. All masses in GeV.

VIII. The ratio ${M_W}^2/\rho_*(0){c_*}^2(Z){M_Z}^2$ as a function of the Z vector boson mass M_Z, the top mass m_t, and the Higgs mass m_H, illustrating the ratio's stability against large radiative corrections. All masses in GeV.

Table I

ρ_* (0)

All masses in GeV: $M_Z = 93$.

	$m_t = 40$	$m_t = 100$	$m_t = 300$	$m_t = 500$	$m_t = 1000$
$m_H = 100$	.9999	1.0025	1.0282	1.0838	1.4517
$m_H = 300$	.9992	1.0018	1.0275	1.0833	1.4534
$m_H = 500$	.9987	1.0013	1.0271	1.0830	1.4546
$m_H = 1000$	.9979	1.0005	1.0264	1.0824	1.4563

Table II

ρ_* (q^2)

All masses in GeV: $M_Z = 93$, $m_H = 100$.

$\sqrt{-q^2}$	$m_t = 40$	$m_t = 100$	$m_t = 300$	$m_t = 500$	$m_t = 1000$
10^{-3}	.999	1.003	1.028	1.084	1.452
10^{-2}	.999	1.003	1.028	1.084	1.452
10^{-1}	.999	1.003	1.028	1.084	1.452
1	.999	1.003	1.028	1.084	1.452
10	1.000	1.003	1.028	1.084	1.452
10^2	1.004	1.006	1.038	1.095	1.466
10^3	1.000	1.000	1.000	1.009	1.284

Table III

G_{μ}. (Z)

$(\times 10^{-5}\ \mathrm{GeV}^{-2})$

All masses in GeV: $M_Z = 93$.

	$m_t = 40$	$m_t = 100$	$m_t = 300$	$m_t = 500$	$m_t = 1000$
$m_H = 100$	1.1526	1.1551	1.1515	1.1514	1.1550
$m_H = 300$	1.1515	1.1540	1.1504	1.1502	1.1538
$m_H = 500$	1.1511	1.1536	1.1500	1.1498	1.1534
$m_H = 1000$	1.1506	1.1530	1.1495	1.1493	1.1529

Table IV

$s^2_*(Z)$

All masses in GeV: $m_H = 100$.

	$m_t = 40$	$m_t = 100$	$m_t = 300$	$m_t = 500$	$m_t = 1000$
$M_Z = 91$	.2348	.2337	.2250	.2089	.1436
$M_Z = 93$	.2210	.2199	.2119	.1972	.1365
$M_Z = 95$	.2086	.2076	.2002	.1866	.1298

Table V

$s^2_*(q^2)$

All masses in GeV: $M_Z = 93$, $m_H = 100$.

$\sqrt{-q^2}$	$m_t = 40$	$m_t = 100$	$m_t = 300$	$m_t = 500$	$m_t = 1000$
10^{-3}	.2297	.2290	.2215	.2076	.1503
10^{-2}	.2296	.2289	.2213	.2074	.1498
10^{-1}	.2295	.2288	.2212	.2072	.1494
1	.2284	.2276	.2200	.2058	.1475
10	.2254	.2246	.2168	.2024	.1429
10^2	.2206	.2196	.2116	.1969	.1362
10^3	.2272	.2266	.2189	.2041	.1403

Table VI

M_W

All masses in GeV: $m_H = 100$.

	$m_t = 40$	$m_t = 100$	$m_t = 300$	$m_t = 500$	$m_t = 1000$
$M_Z = 91$	79.541	79.779	81.402	84.490	101.797
$M_Z = 93$	82.026	82.260	83.896	86.997	104.491
$M_Z = 95$	84.457	84.686	86.343	89.465	107.168

Table VII

M_W

All masses in GeV: $m_t = 40$.

	$m_H = 100$	$m_H = 300$	$m_H = 500$	$m_H = 1000$
$M_Z = 91$	79.541	79.476	79.441	79.390
$M_Z = 93$	82.026	81.962	81.928	81.878
$M_Z = 95$	84.457	84.395	84.361	84.312

Table VIII

$M_W^2/\rho_*(0)c_*^2(Z)M_Z^2$

All masses in GeV: $m_H = 100$.

	$m_t = 40$	$m_t = 100$	$m_t = 300$	$m_t = 500$	$m_t = 1000$
$M_Z = 91$	.9985	1.0005	1.0042	1.0054	1.0064
$M_Z = 93$	.9987	1.0030	1.0043	1.0057	1.0071
$M_Z = 95$	.9987	1.0003	1.0045	1.0060	1.0075

All masses in GeV: $m_t = 40$.

	$m_H = 100$	$m_H = 300$	$m_H = 500$	$m_H = 1000$
$M_Z = 91$	.9985	.9985	.9985	.9985
$M_Z = 93$	.9987	.9985	.9986	.9987
$M_Z = 95$	.9987	.9987	.9986	.9986

FIGURE CAPTIONS

1. Oblique corrections.
2. Direct corrections: vertices, boxes, bremsstrahlung.
3. Higher-order vacuum polarization.
4. Higher-order nonoblique correction.
5. Four-fermion electroweak process.
6. Neutral-current electroweak Dyson's equations.[9]
7. Charged-current electroweak Dyson's equations.[9]
8. Non–Abelian vertices.
9. Longitudinal Π_{3Q}, proportional to non–Abelian vertex.
10. Vector boson self-energies due to vector boson parts: loops, tadpoles, ghosts, would-be Goldstones, and mixed diagrams.
11. $4\pi/e_*^2\ (q^2)$ a. timelike; b. spacelike 1 MeV to 1 TeV.
12. $s_*^2\ (q^2)$ a. timelike; b. spacelike 1 MeV to 1 TeV.
13. $\rho_*\ (0)$ versus top mass m_t in GeV.
14. $\rho_*\ (0)$ versus Higgs mass m_H in GeV.
15. $\rho_*\ (q^2)$ timelike 1 MeV to 1 TeV versus top mass m_t in GeV.
16. $G_{\mu *}\ (Z)$ versus a common top/bottom mass in GeV.
17. $G_{\mu *}\ (Z)$ versus top mass m_t and Higgs mass m_H in GeV.
18. $G_{\mu *}\ (q^2)$ timelike 1 MeV to 1 TeV.
19. $s_*^2\ (Z)$ and $s_*^2\ (0)$ versus top mass m_t in GeV.
20. $s_*^2\ (q^2)$ timelike 1 MeV to 1 TeV versus top mass m_t in GeV.
21. $s_*^2\ (Z)$ and $s_*^2\ (0)$ versus Higgs mass m_H in GeV.

22. $s_*^2\ (Z)$ versus Z mass M_Z and top mass m_t in GeV.

23. $s_*^2\ (Z)$ versus Z mass M_Z and Higgs mass m_H in GeV.

24. W mass M_W versus Z mass M_Z and top mass m_t in GeV.

25. W mass M_W versus Z mass M_Z and Higgs mass m_H in GeV.

26. Experimental uncertainty in A_{LR} and $s_*^2\ (Z)$.[25]

27. Z width $\Gamma_*\ (Z)$ versus top mass m_t in GeV.

28. $\kappa_*\ (Z)$ versus top mass m_t in GeV.

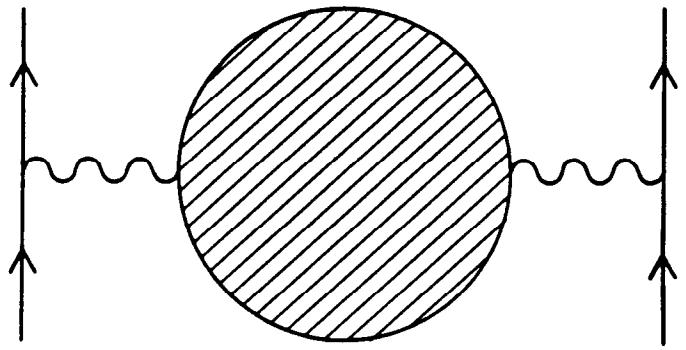

6-87 5796A1

Fig. 1

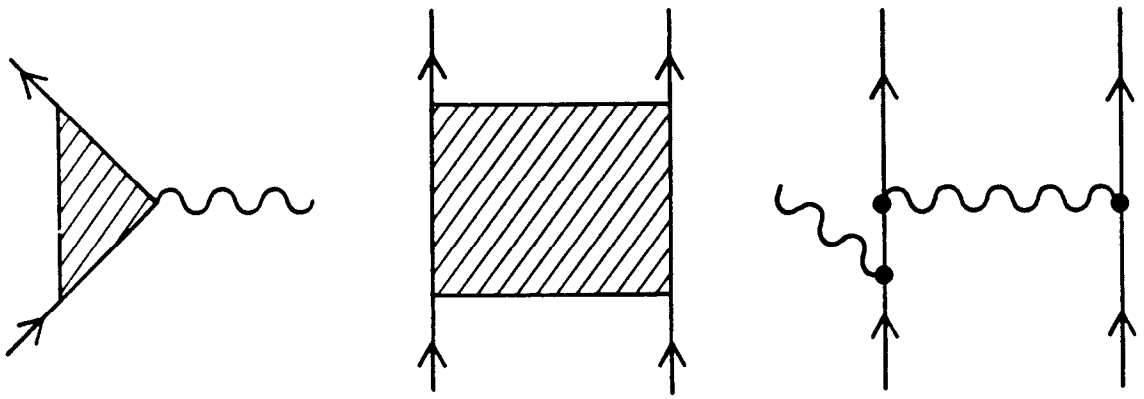

6-87

5796A2

Fig. 2

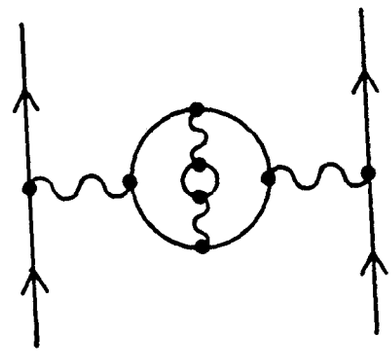

6-87 5796A3

Fig. 3

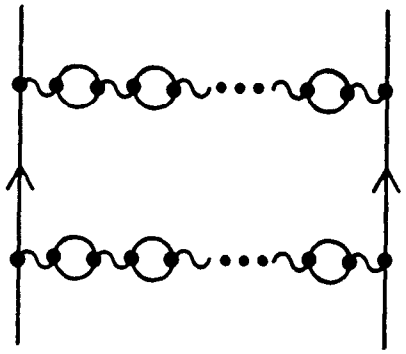

6-87 5796A4

Fig. 4

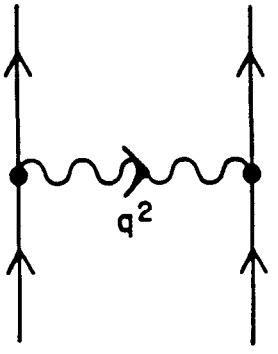

6-87 5796A8

Fig. 5

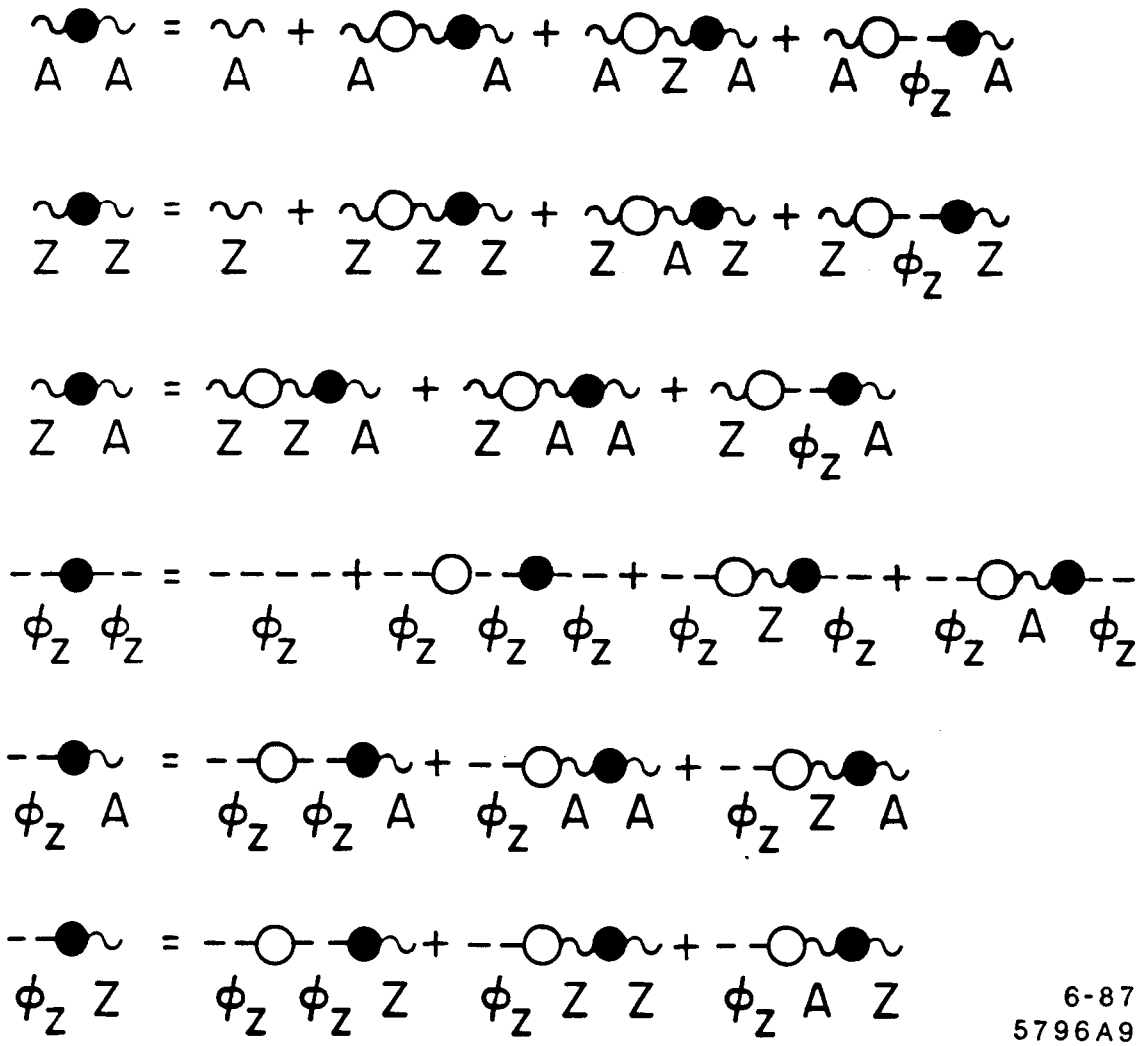
A A = A + A + A + A Z A + A ϕ_z A
Z Z = Z + Z Z Z + Z A Z + Z ϕ_z Z
Z A = Z Z A + Z A A + Z ϕ_z A
ϕ_z ϕ_z = ϕ_z + ϕ_z ϕ_z ϕ_z + ϕ_z Z ϕ_z + ϕ_z A ϕ_z
ϕ_z A = ϕ_z ϕ_z A + ϕ_z A A + ϕ_z Z A
ϕ_z Z = ϕ_z ϕ_z Z + ϕ_z Z Z + ϕ_z A Z
6-87
5796A9

Fig. 6

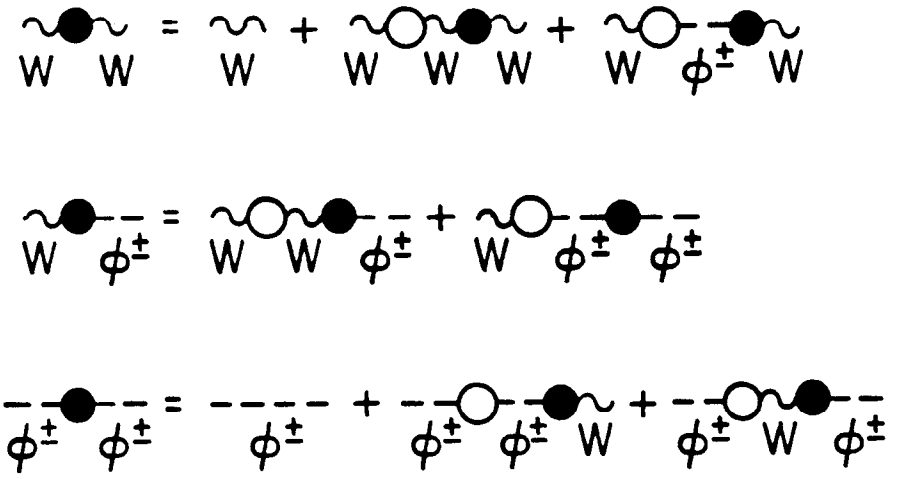

6-87 5796A10

Fig. 7

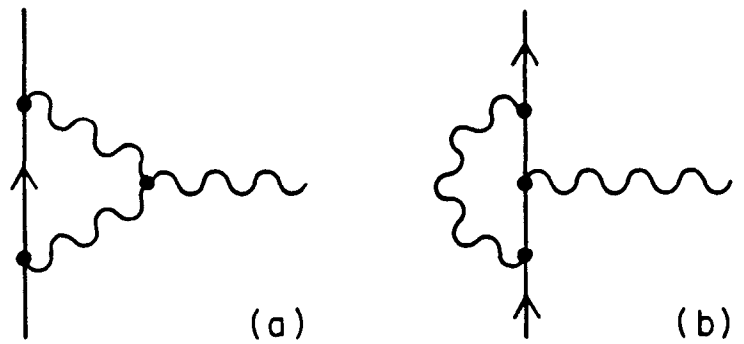

6-87 5796A5

Fig. 8

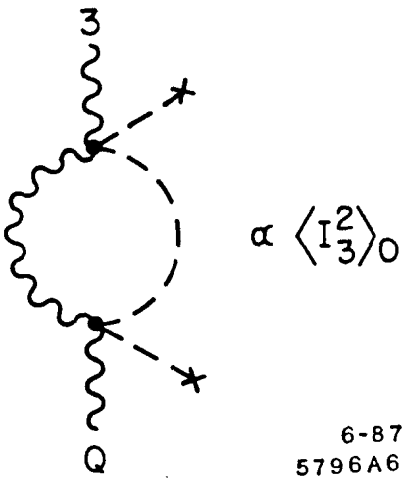

Fig. 9

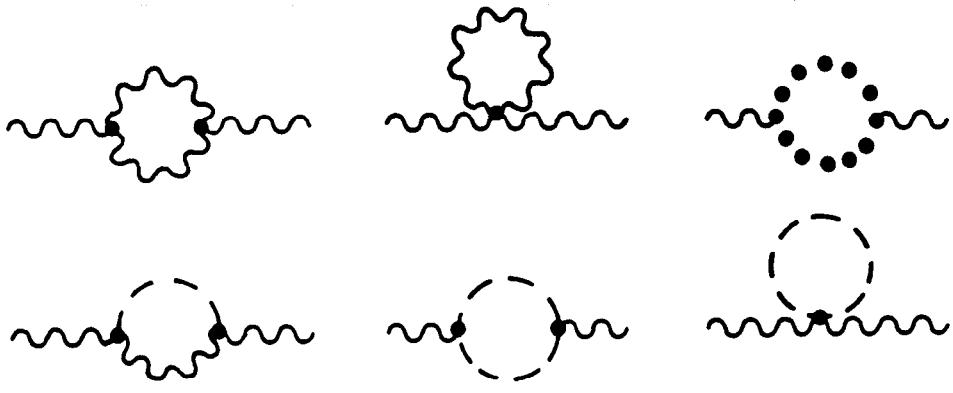

6-87 5796A7

Fig. 10

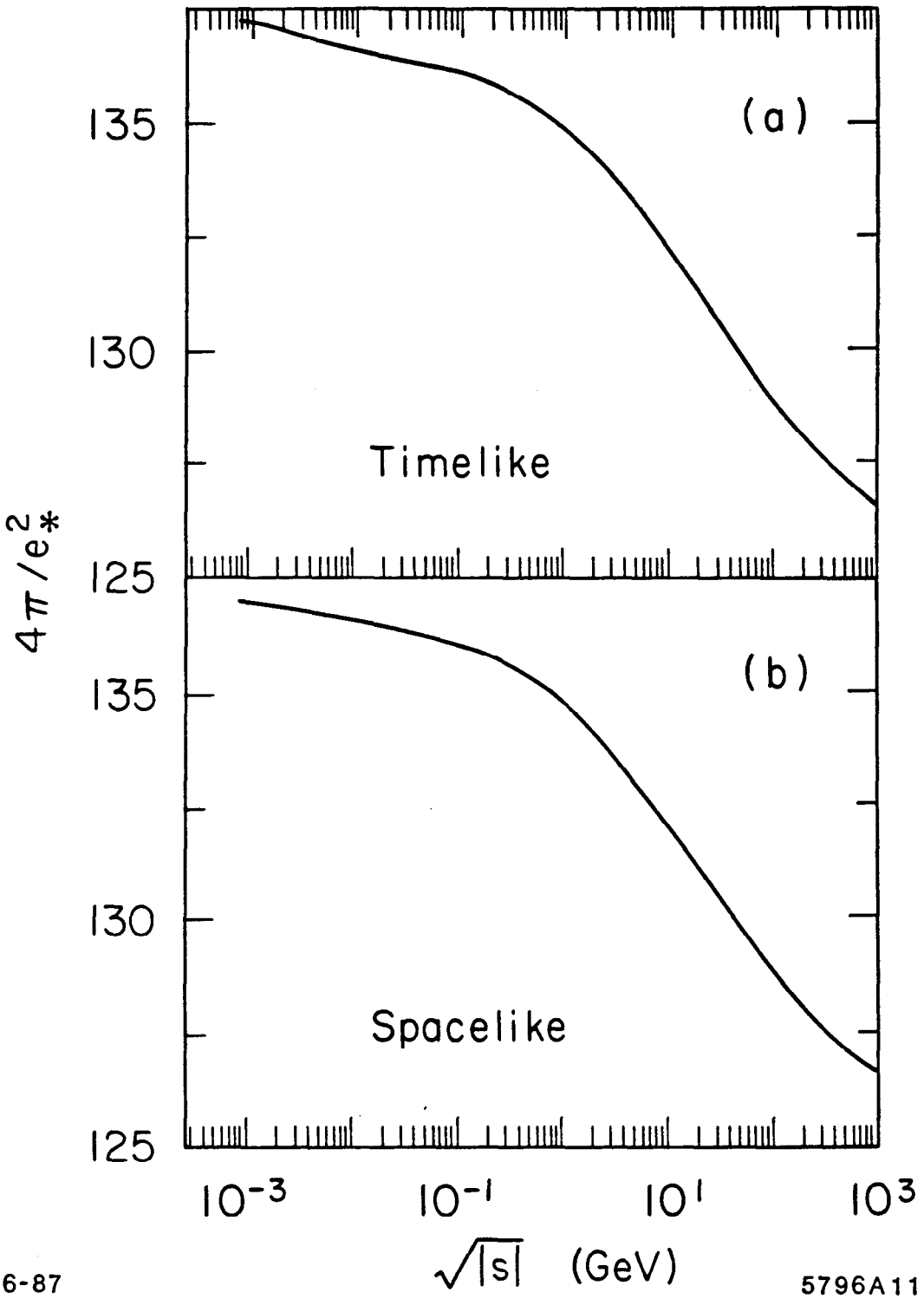
135
130
125
(a)
Timelike
$4\pi/e^2*$
135
130
125
(b)
Spacelike
10^{-3}
10^{-1}
10^{1}
10^{3}
$\sqrt{|s|}$ (GeV)
6-87
5796A11

Fig. 11

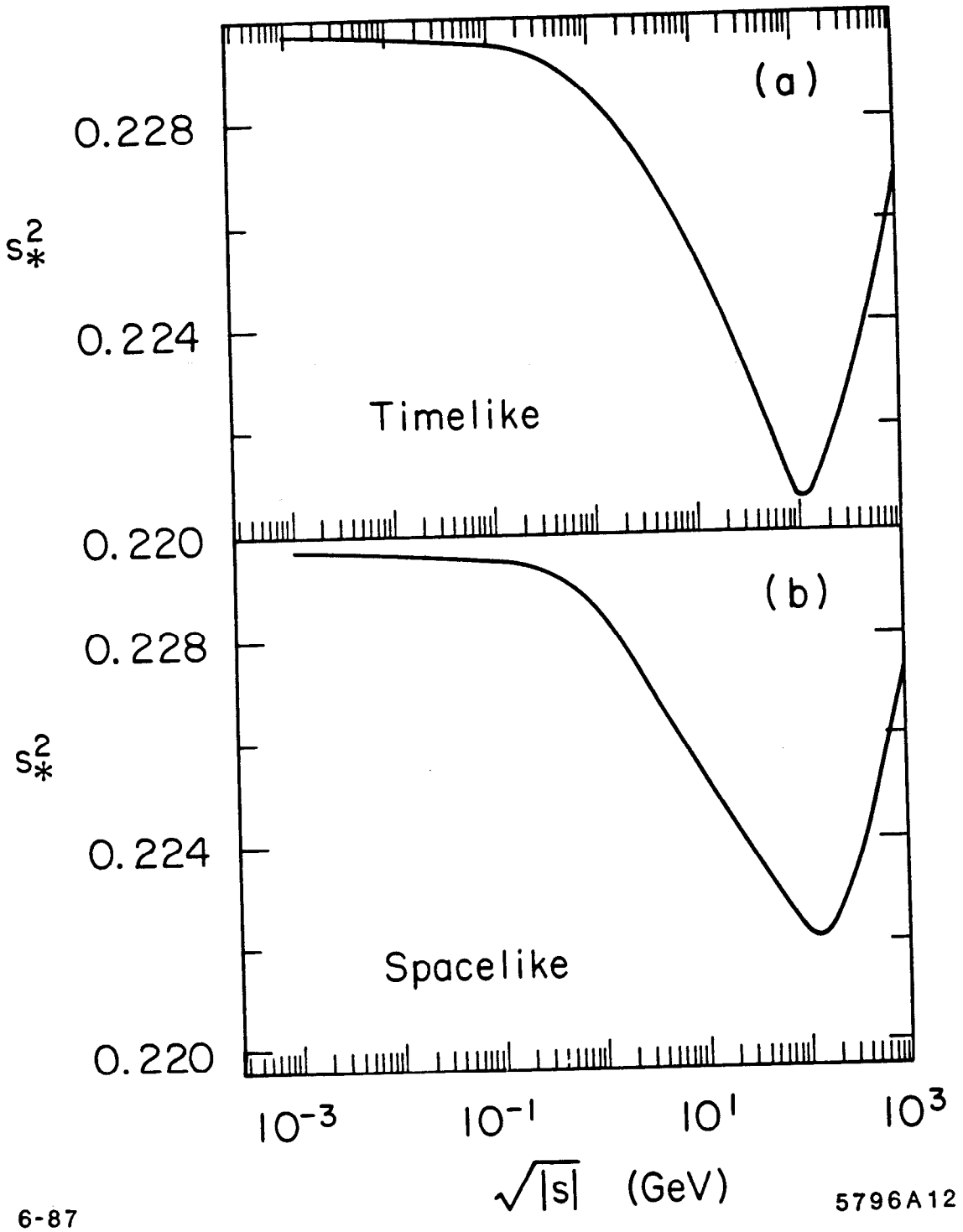
(a)
0.228
s^2_*
0.224
Timelike
0.220
(b)
0.228
s^2_*
0.224
Spacelike
0.220
10^{-3}
10^{-1}
10^{1}
10^{3}
$\sqrt{|s|}$ (GeV)
5796A12

6-87

Fig. 12

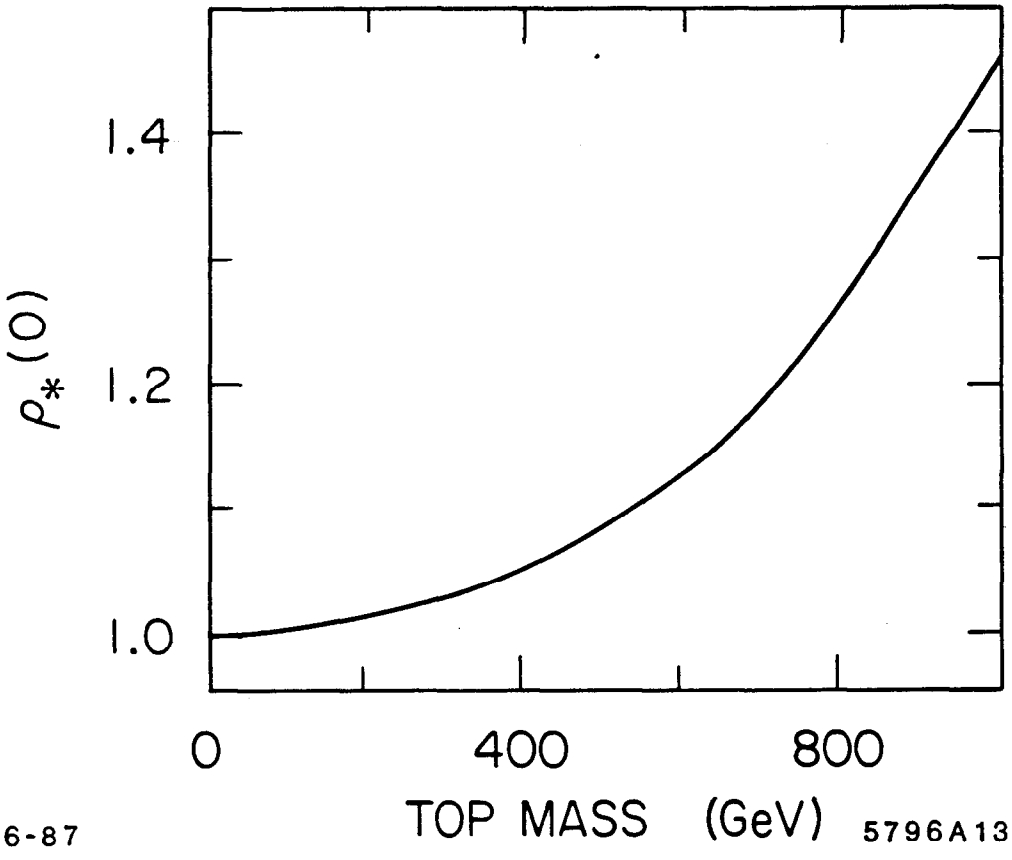

Fig. 13

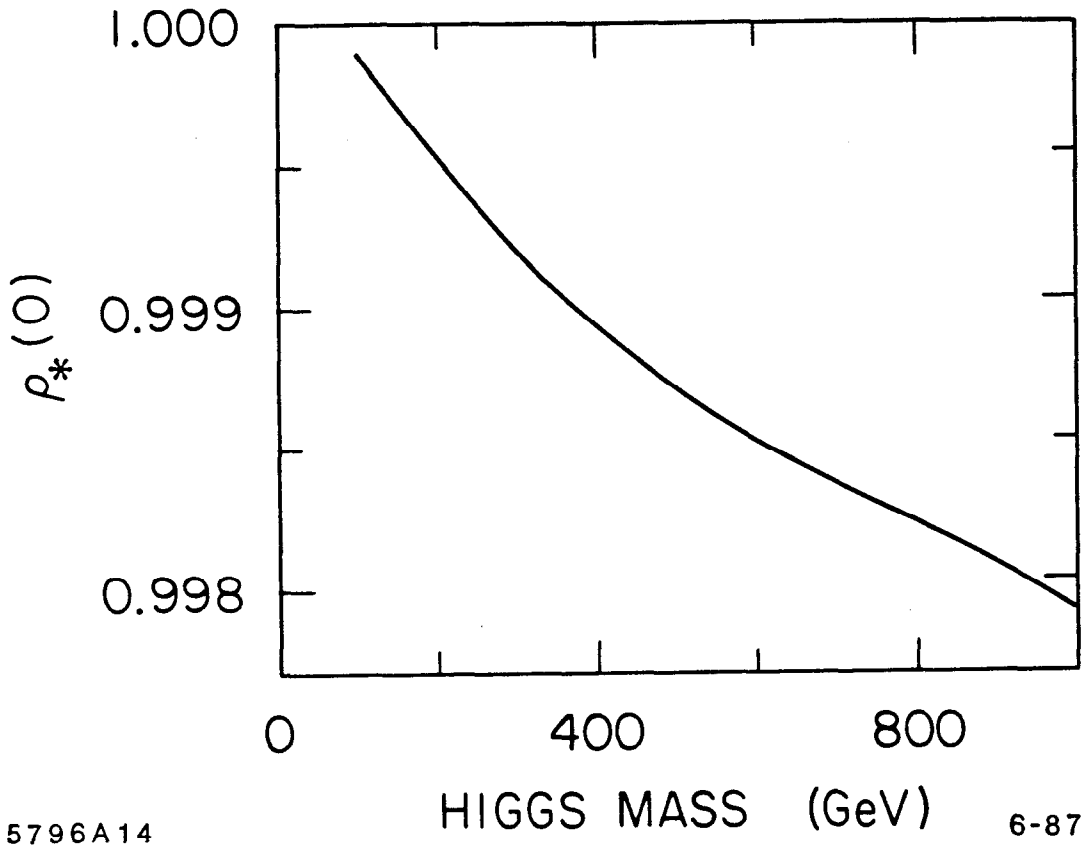

Fig. 14

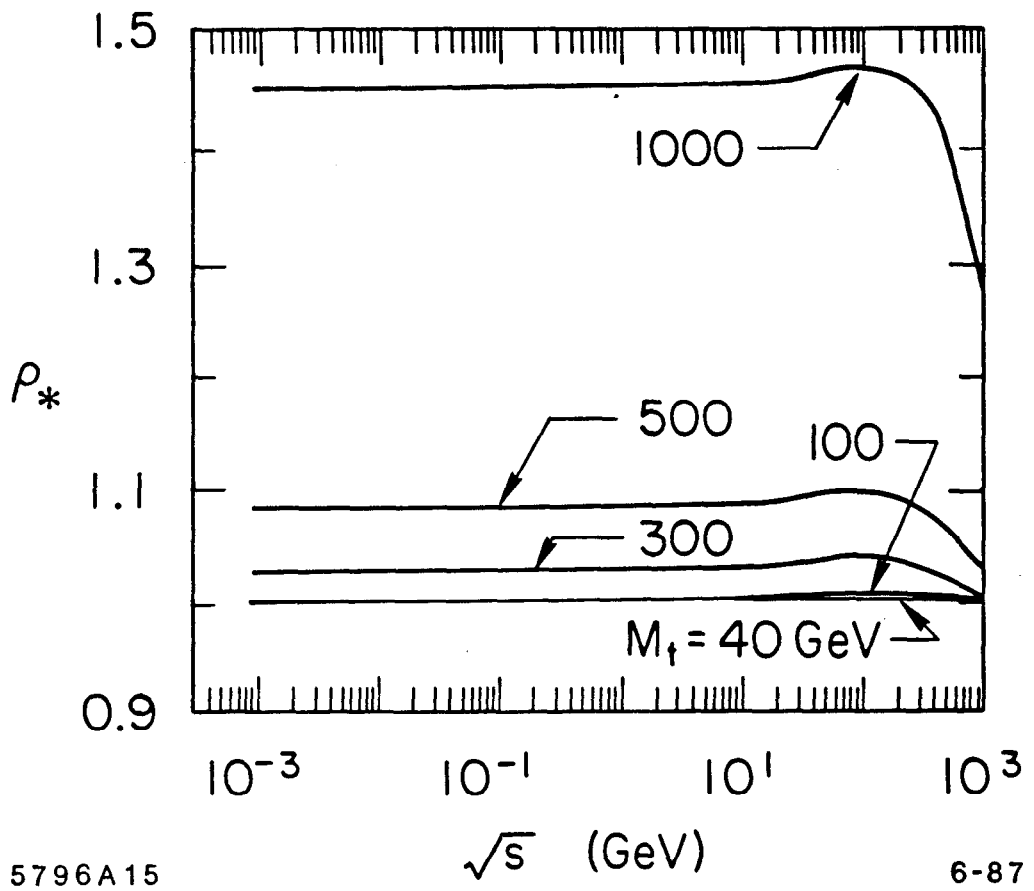
1.5
1.3
1.1
0.9
ρ_*
1000
500
100
300
$M_t = 40$ GeV
10^{-3}
10^{-1}
10^{1}
10^{3}
$\sqrt{s}$ (GeV)
5796A15
6-87

Fig. 15

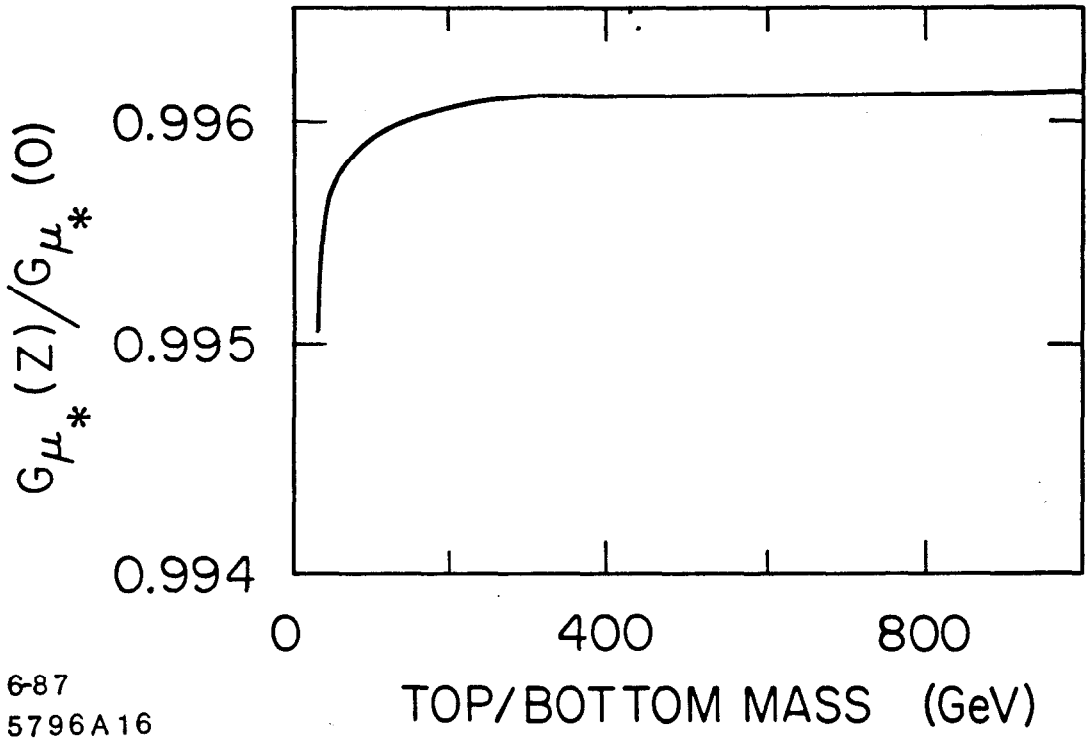
0.996
0.995
0.994
$G_{\mu^*}(Z)/G_{\mu^*}(0)$
0
400
800
TOP/BOTTOM MASS (GeV)
6-87
5796A16

Fig. 16

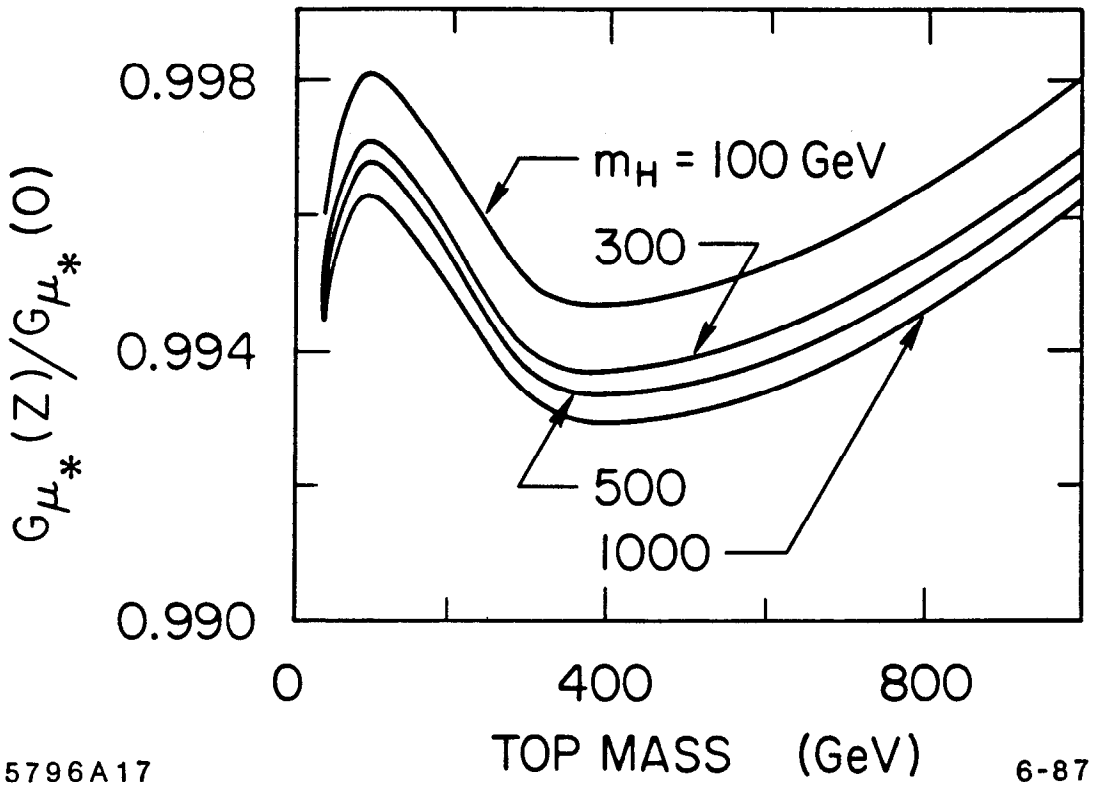
0.998
0.994
0.990
$G_{\mu^*}(Z)/G_{\mu^*}(0)$
m_H = 100 GeV
300
500
1000
0
400
800
TOP MASS (GeV)
5796A17
6-87

Fig. 17

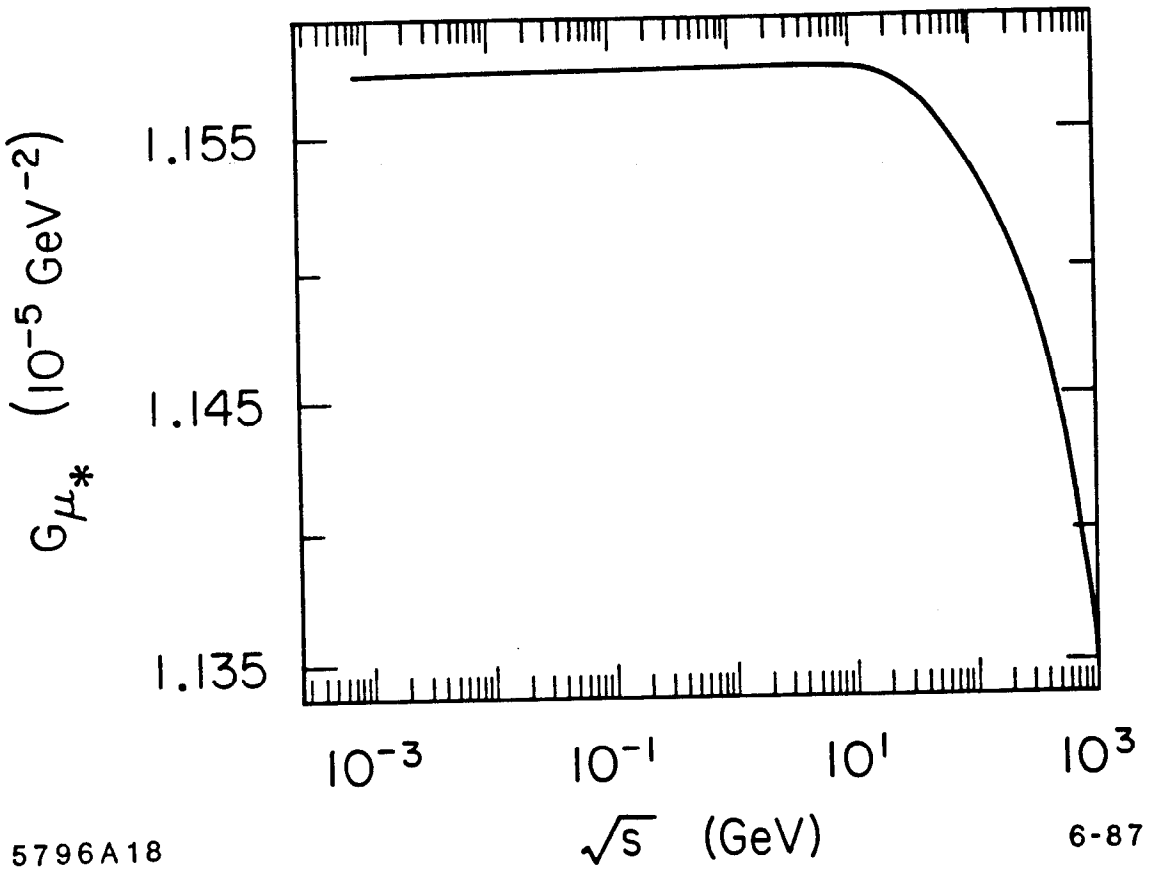
G_{μ^*} $(10^{-5}\ GeV^{-2})$
1.155
1.145
1.135
10^{-3}
10^{-1}
10^{1}
10^{3}
$\sqrt{s}$ (GeV)
5796A18
6-87

Fig. 18

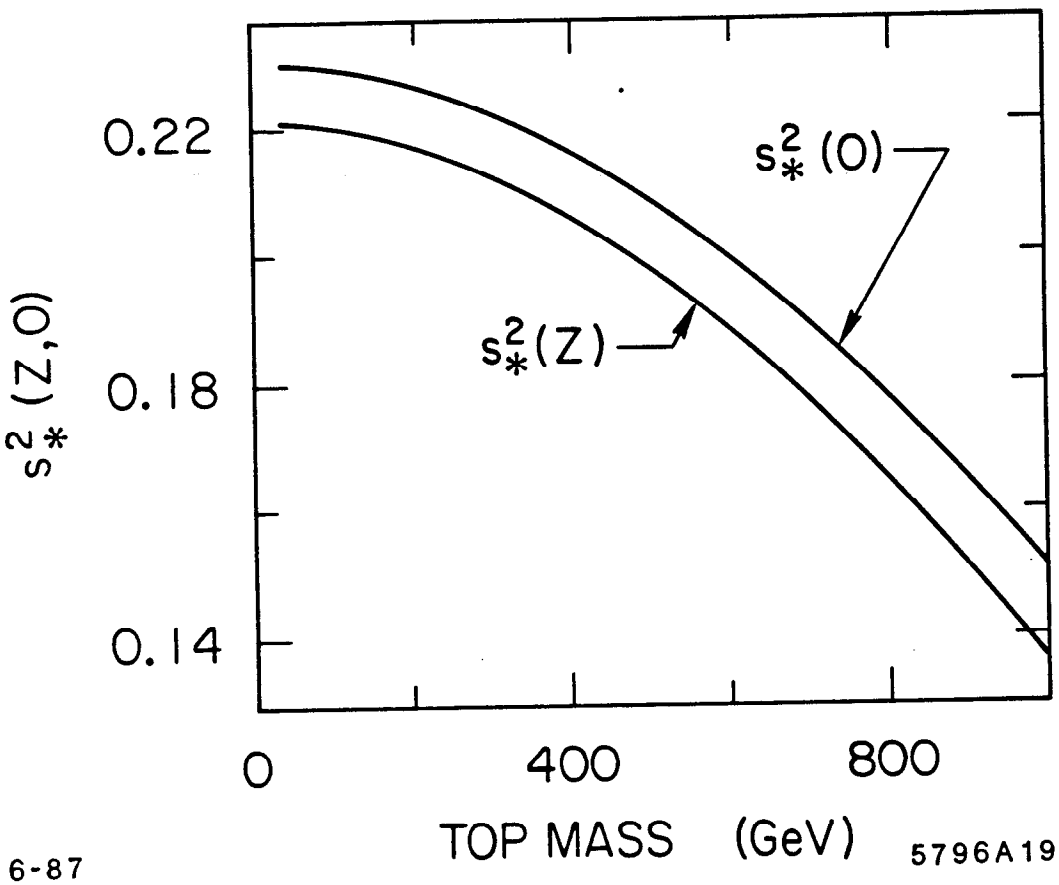

Fig. 19

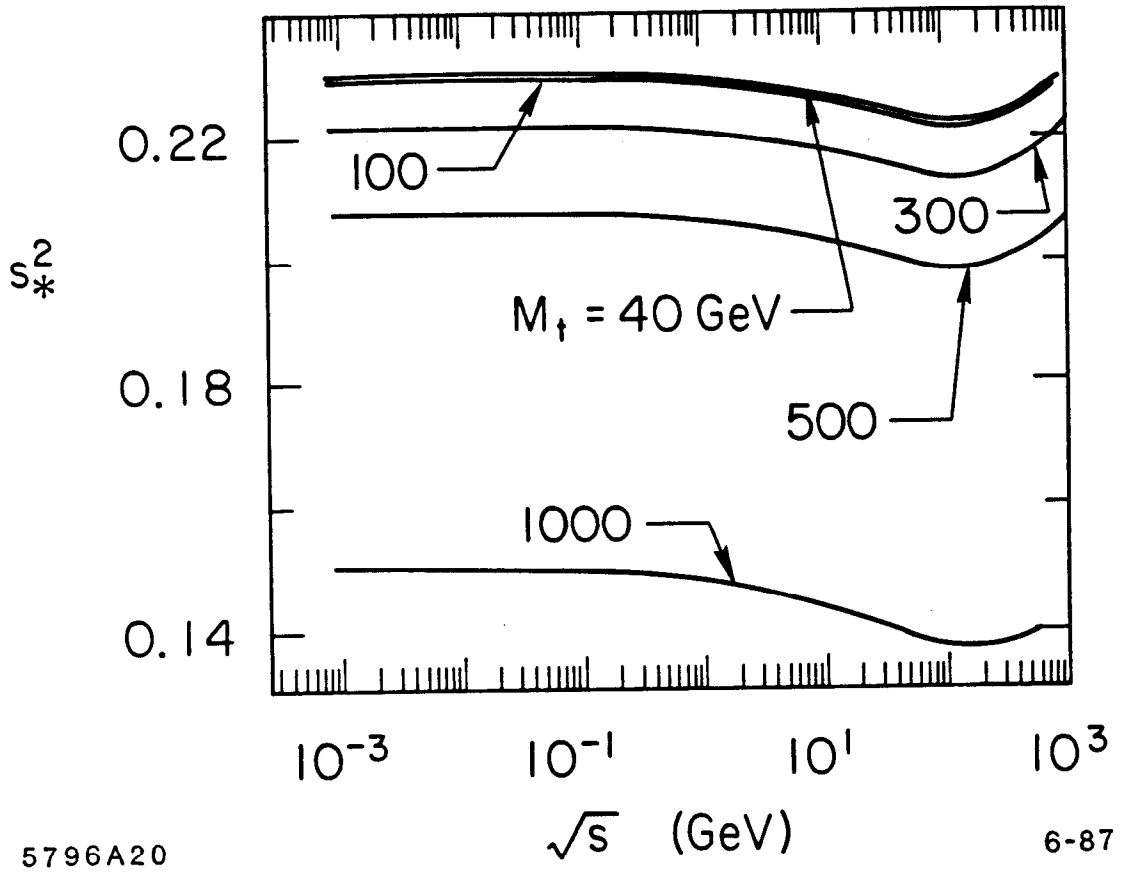
0.22
0.18
0.14
s^2_*
100
300
M_t = 40 GeV
500
1000
10^{-3}
10^{-1}
10^{1}
10^{3}
$\sqrt{s}$ (GeV)
5796A20
6-87

Fig. 20

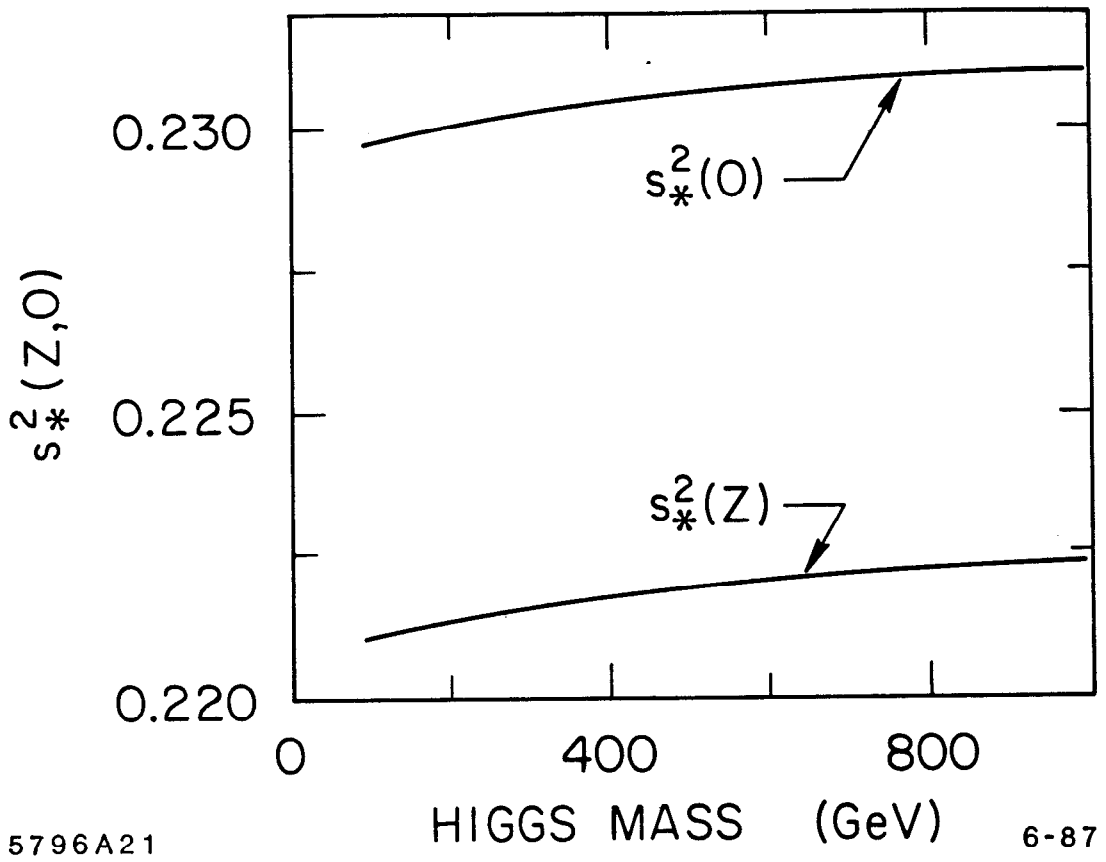
0.230
0.225
0.220
$s^2_*(Z,0)$
$s^2_*(0)$
$s^2_*(Z)$
0
400
800
HIGGS MASS (GeV)
5796A21
6-87

Fig. 21

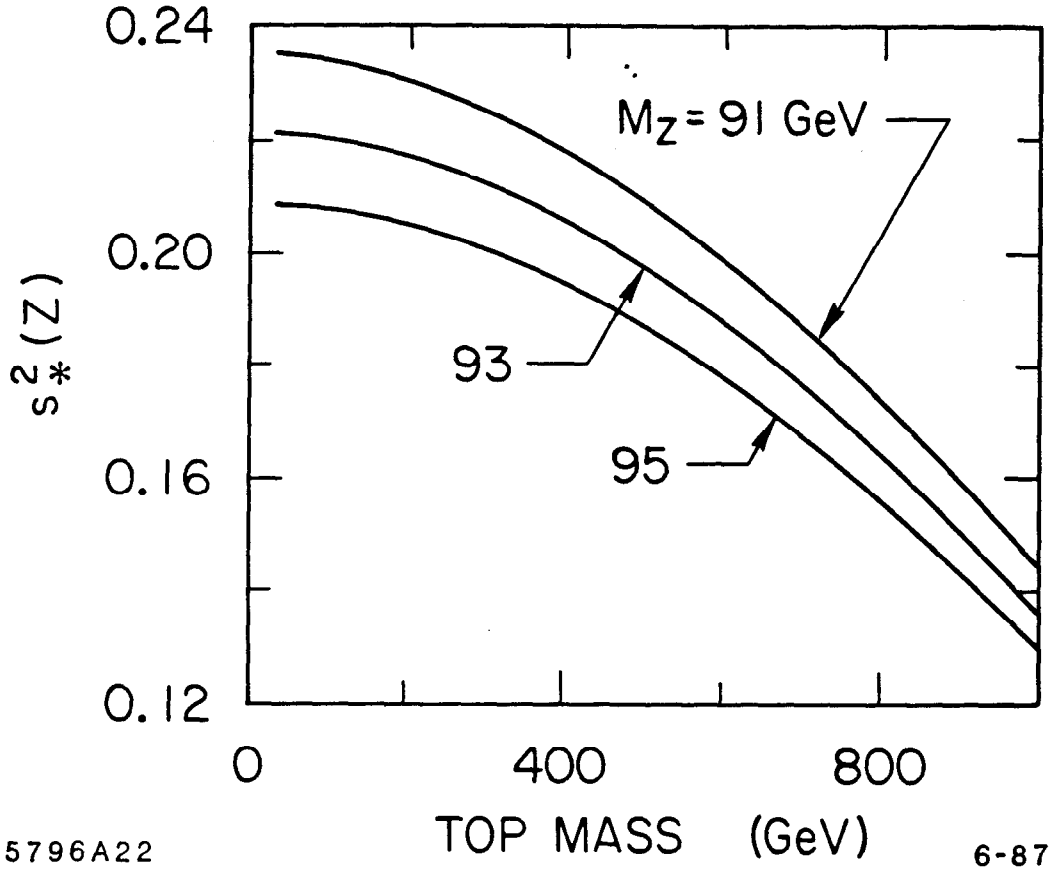
0.24
0.20
0.16
0.12
$s^2_*(Z)$
M_Z = 91 GeV
93
95
0
400
800
TOP MASS (GeV)
5796A22
6-87

Fig. 22

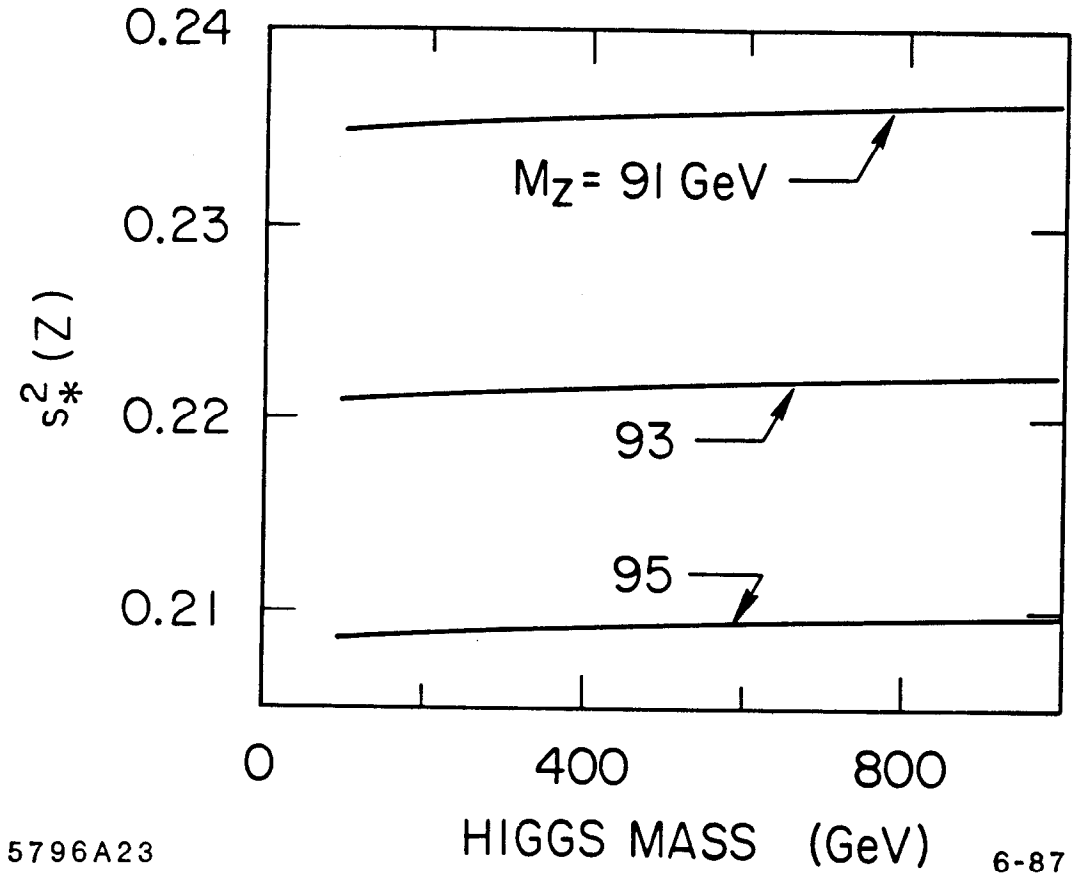
0.24
0.23
0.22
0.21
$s^2_*(Z)$
M_Z = 91 GeV
93
95
0
400
800
HIGGS MASS (GeV)
5796A23
6-87

Fig. 23

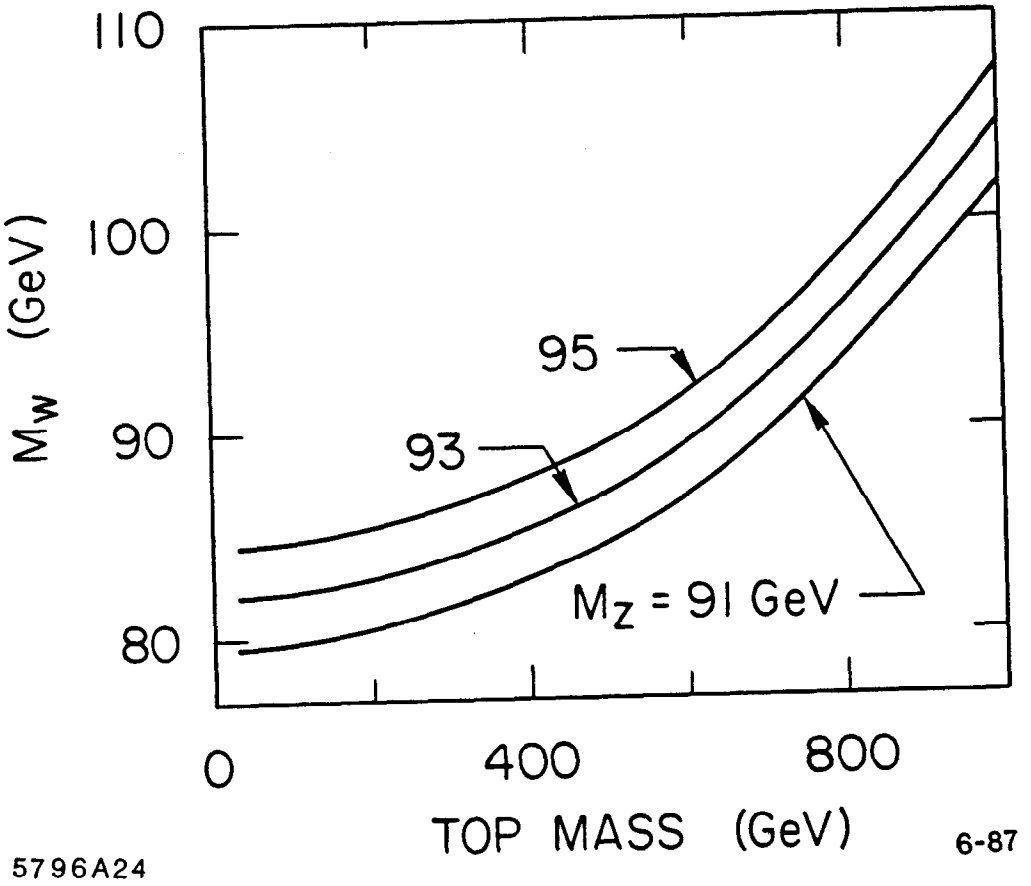
110
100
90
80
M_W (GeV)
95
93
M_Z = 91 GeV
0
400
800
TOP MASS (GeV)
5796A24
6-87

Fig. 24

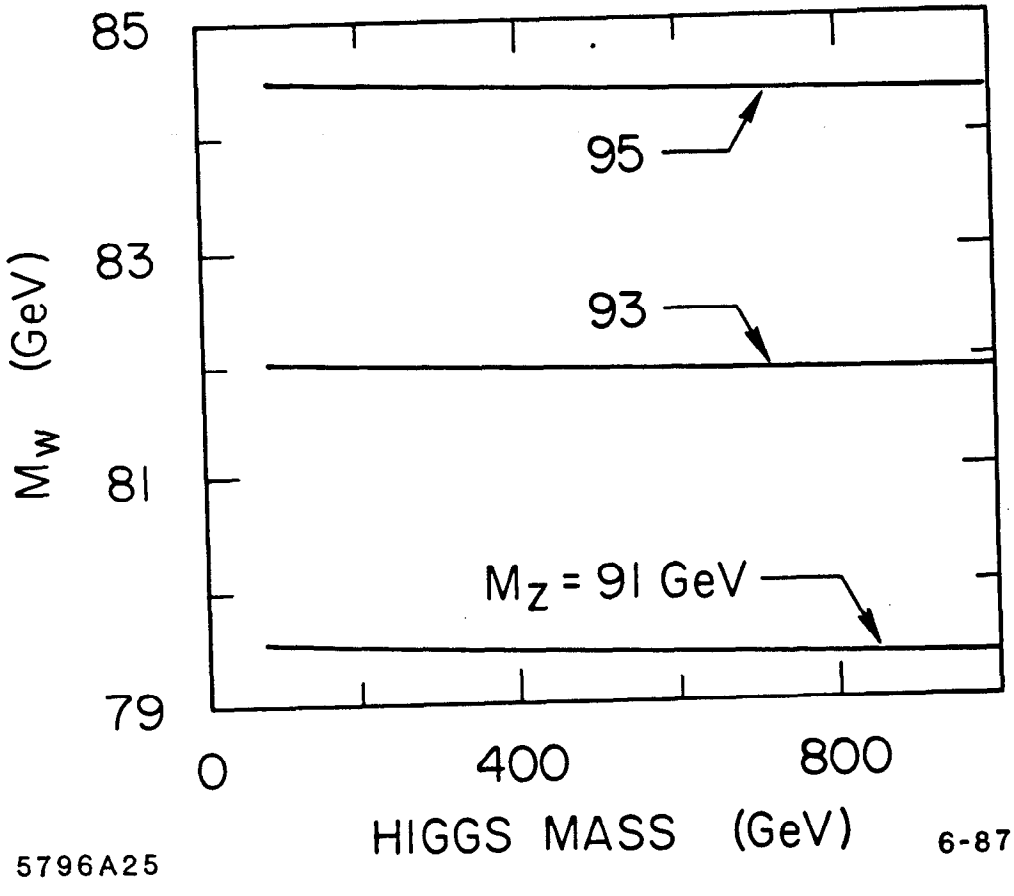
85
83
81
79
M_W (GeV)
95
93
M_Z = 91 GeV
0
400
800
HIGGS MASS (GeV)
5796A25
6-87

Fig. 25

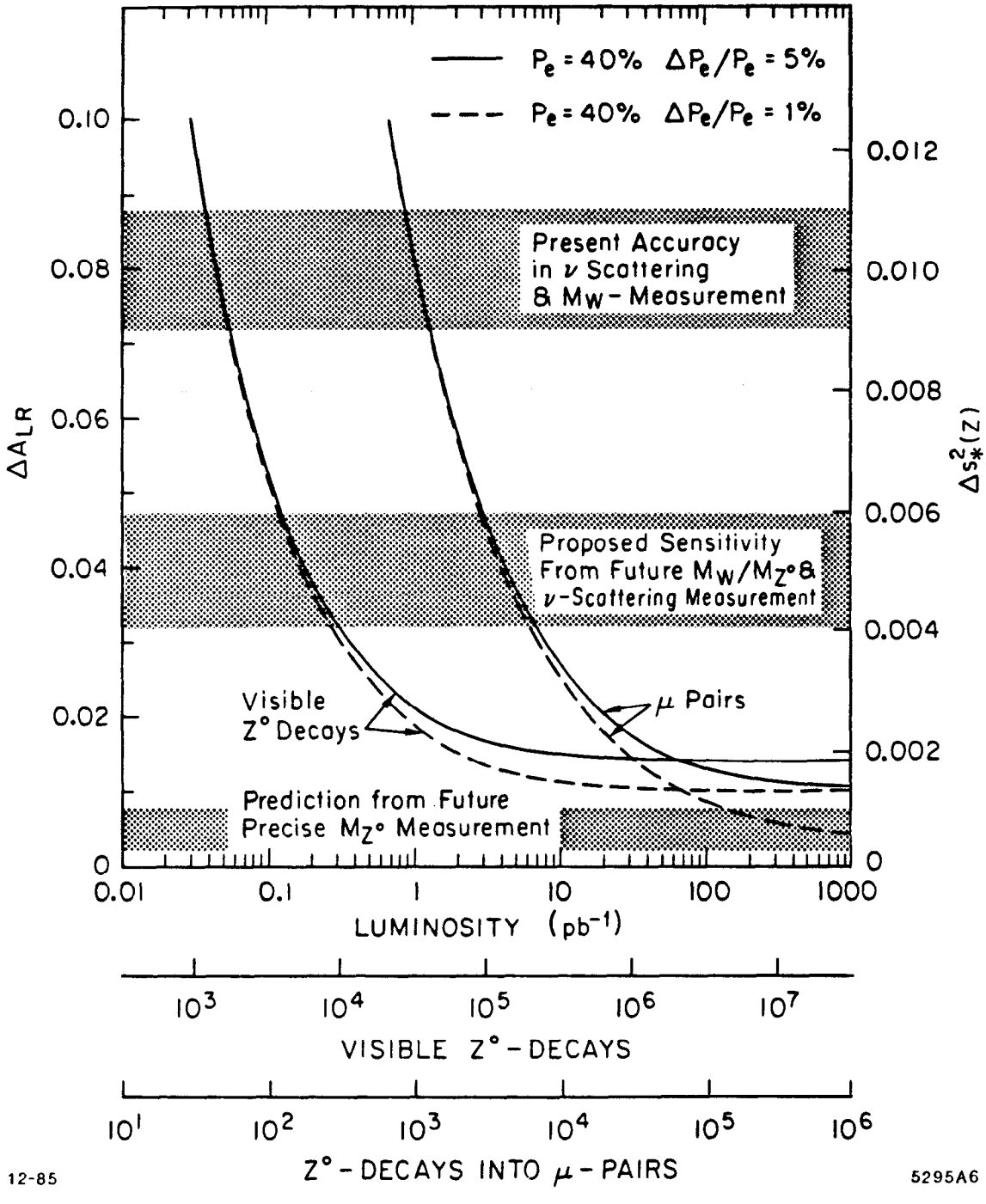
$P_e = 40\%$ $\Delta P_e/P_e = 5\%$
$P_e = 40\%$ $\Delta P_e/P_e = 1\%$
Present Accuracy in ν Scattering & M_W - Measurement
Proposed Sensitivity From Future M_W/M_{Z^0} & ν-Scattering Measurement
Visible Z^0 Decays
μ Pairs
Prediction from Future Precise M_{Z^0} Measurement
ΔA_{LR}
$\Delta s^2_*(Z)$
0.10
0.08
0.06
0.04
0.02
0
0.012
0.010
0.008
0.006
0.004
0.002
0
0.01
0.1
1
10
100
1000
LUMINOSITY (pb^{-1})
10^3
10^4
10^5
10^6
10^7
VISIBLE Z^0 - DECAYS
10^1
10^2
10^3
10^4
10^5
10^6
Z^0 - DECAYS INTO μ - PAIRS
12-85
5295A6

Fig. 26

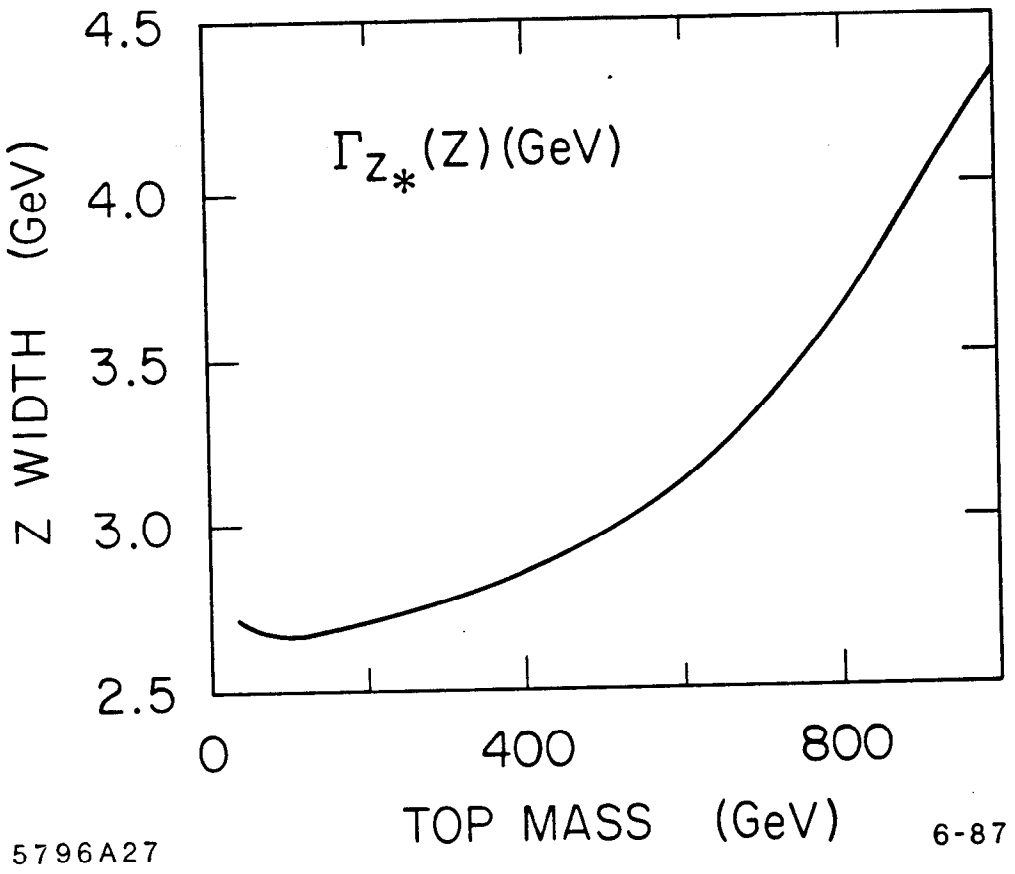
4.5
4.0
3.5
3.0
2.5
Z WIDTH (GeV)
$\Gamma_{Z_*}(Z)$(GeV)
0
400
800
TOP MASS (GeV)
5796A27
6-87

Fig. 27

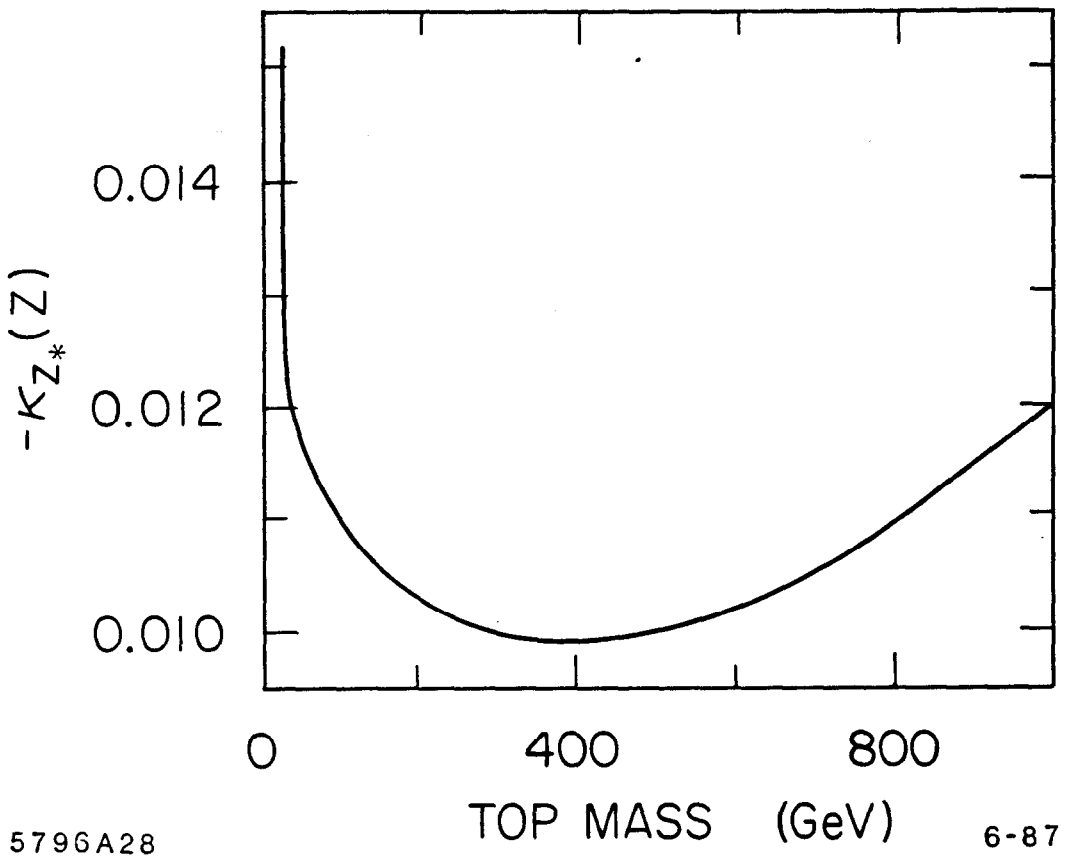

Fig. 28